Stochastic nuclear dynamics

Yu. L. Bolotin, V. Yu. Gonchar, E. V. Inopin, V. V. Levenko, V. N. Tarasov, and N. A. Chekanov

Khar'kov Physicotechnical Institute, Ukrainian Academy of Sciences, Khar'kov

Fiz. Elem. Chastits At. Yadra **20**, 878–929 (July–August 1989)

The transition from regular to random motion is studied for collective nuclear processes with large amplitude. The connection between the features of the dynamics and the geometry of the potential-energy surface is studied. Some two-dimensional dynamical systems, including quadrupole surface vibrations of nuclei and induced nuclear fission, are studied in detail. Some quantum manifestations of classical stochasticity are investigated, in particular the connection between the statistical properties of the quantum energy spectra and the nature of the motion—regular or random—in the classical limit. For potentials with a localized region of negative Gaussian curvature there is found to be a triple transition: regularity–chaos–regularity, and its influence on the statistical properties of the spectrum is investigated.

INTRODUCTION

Collective nuclear motions of large amplitude, leading to a radical rearrangement of the ground state, yield important information about the structure of nuclear matter and the interaction of the nucleons in it. However, to describe such collective motions theoretically it is necessary to go beyond the traditional methods, which are based largely on linear approximations. In addition, the overwhelming majority of the problems that can be solved in nuclear physics are one-dimensional or are artificially reduced to such problems by the use of an approximate symmetry of the problem or the separation of some dominant degree of freedom (such as the fission coordinate in the description of fission) and the neglect of "secondary" degrees of freedom. It is assumed tacitly that allowance for the neglected degrees of freedom cannot radically change the results of the one-dimensional problem.

The treatment of the nucleus as a multidimensional nonlinear dynamical system (described, in particular, by Hamiltonian equations of motion) permits the existence, under certain conditions, of not only the well-studied regular solutions of the equations, of motion but also fundamentally new dynamical regimes for which the motion of the nuclear matter is indistinguishable from a stochastic motion even though there is absolutely no external source of stochasticity.[1-4] Using for the epithet *random* the synonyms *chaotic* and *stochastic*, we can assert that for the nucleus, as for any nonlinear dynamical system, these concepts adequately reflect certain fundamental intrinsic properties which represent an important and interesting subject of investigation.

Collective excitations of nuclei are traditionally described in the framework of phenomenological models,[5,6] in which nuclear matter is treated as a fluid possessing definite properties of inertia, elasticity, and viscosity. Each such model is adapted to the description of just a few experiments and requires the introduction of a set of parameters whose relation to the original nucleon–nucleon interaction is outside the scope of the model. The assumption that the collective motions are adiabatic, i.e., that the collective velocities are small compared with the single-particle velocities of the nucleons in the nucleus, permits an expansion of the total energy in a series in which a restriction is made to the terms quadratic in the collective velocities and, thus, a casting of the Hamiltonian into the form that is usually postulated in phenomenological models:

$$H(\mathbf{p}, \mathbf{q}) = \frac{p^2}{2m} + U(\mathbf{q}), \tag{1}$$

where $\mathbf{q}$ is the collective coordinate, and $\mathbf{p}$ is its canonically conjugate momentum. However, in contrast to phenomenological models, the parameters of the adiabatic collective Hamiltonian are directly related to the original effective interaction of the nucleons in the nucleus. The dynamics of the collective motions is determined, in general, by a nonlinear nonseparable collective potential $U(\mathbf{q})$. By means of a canonical transformation $(\mathbf{p},\mathbf{q}) \Rightarrow (\mathbf{P},\mathbf{Q})$, the Hamiltonian (1) can be reduced to the form

$$H(\mathbf{P}, \mathbf{Q}) = H_0(\mathbf{P}, \mathbf{Q}) + \varepsilon V(\mathbf{P}, \mathbf{Q}), \quad \varepsilon \ll 1, \tag{2}$$

where H_0 is an integrable Hamiltonian, and V is a nonlinear and nonintegrable correction.

The classical concept of integrability, which derives from Poincaré, relates this property to the existence, alongside the energy, of additional single-valued integrals of the motion, which correspond to a "hidden" symmetry of the problem. More rigorously, Liouville's theorem[7] states that a Hamiltonian system with N degrees of freedom is integrable if there exist N single-valued integrals of the motion in involution. In other words,[8] the property of integrability is tantamount to the possibility of decomposing the motion into elementary components. In the integrable case, motion on a torus is an elementary dynamical component, and it can be conveniently described in angle–action variables. In these variables, the Hamiltonian (2) takes the form

$$H(\mathbf{I}, \theta) = H_0(\mathbf{I}) + \varepsilon V(\mathbf{I}, \theta). \tag{3}$$

The prediction of the behavior of a nonlinear system described by such a Hamiltonian (Poincaré regarded this problem as the main problem of dynamics[7]) was traditionally based on one of the following two versions. According to the first, the weak (as measured by the small ε) perturbation leads merely to a small shift of the frequencies and to the appearance of small combination harmonics. In this case, as in the exactly integrable case, the system is characterized by N integrals of the motion, though admittedly they are now approximate. But the second version supposes that even a weak perturbation can lead to a significant distortion of the

 0090-4759/89/040372-21$04.40

unperturbed motion, destroying the corresponding integrals of the motion and transforming it into stochastic motion. While the first approach appeared natural, the adoption of the second, at least for systems with a small number of degrees of freedom, encountered difficulties. The last 30 years has witnessed the difficult recognition that stochastic motion is as common a phenomenon in systems with more than one degree of freedom as is ordinary quasiperiodic motion. Examples of stochastic motion have been found in practically all branches of physics,[1-4] and their number is increasing steadily all the time.

The mechanism which ensures the existence of stochastic regimes in strictly deterministic systems is local instability. This has the consequence that initially neighboring trajectories separate exponentially in the phase space:

$$d(t) = d(0)\, e^{ht}, \tag{4}$$

where d is the distance between two points in the phase space belonging to different trajectories. More precisely, by stochasticity one can understand the appearance in the system of statistical properties on account of local instability.

Let $f(z)$ and $g(z)$ be two arbitrary functions of the coordinate $z(t) = [q(t), p(t)]$ in the phase space. The evolution of the system is determined by an operator $\hat{T}$,

$$\hat{T}\, z(t) = z(t + T), \tag{5}$$

and the evolution of an arbitrary function of z can be represented in the form

$$f(z, t + T) \equiv \hat{S}_T\, f(z, t) = f(\hat{T}\, z, t). \tag{6}$$

We define the correlation function

$$R(f, g \mid T) = \langle \hat{S}_T\, f, g \rangle - \langle f \rangle \langle g \rangle, \tag{7}$$

where $\langle f \rangle \equiv \int f(z)\, d\mathbf{p}d\mathbf{q}$. One can show[1] that from the local-instability property (4) there follows the property of mixing—the destruction of the correlations:

$$\lim_{T \to \infty} R(f, g \mid T) \sim e^{-h_c t}. \tag{8}$$

Moreover, the growth rate $\langle h \rangle$ of the local instability determines the correlation decoupling time:

$$h_c \sim \langle h \rangle. \tag{9}$$

This relation establishes the connection between the dynamics of the system and its statistical properties.

The local instability of the trajectories makes the problem of specifying the initial conditions in classical mechanics as fundamental as the uncertainty principle, i.e., the problem of measurements in quantum mechanics. The traditional determinism of classical mechanics, based on identification of the physical world with a mathematical continuum, presupposes the possibility of specifying initial conditions with absolute accuracy, a manifest nonsense. "It has always seemed to me remarkable that there should exist a domain—mechanics—and a classical physics formed in its image in which everything is absolutely exact and free of the uncertainties that usually control life and human thought. Therefore, I see the elimination of the imaginary accuracy realized by modern physics as progress in the effort to achieve a unified view of the world... . It would be sensible to formulate classical mechanics too in a statistical form from the very beginning."[9] For systems subject to local instability a statistical description is the only one possible.

The foregoing general considerations are confirmed by direct observation of random regimes in the mathematical modeling of nuclear reactions with heavy ions[10]:

$$^4\mathrm{He} + {}^{14}\mathrm{C};\ {}^{12}\mathrm{C} + {}^{12}\mathrm{C}\ (0^+);\ {}^4\mathrm{He} + {}^{20}\mathrm{Ne}.$$

The authors of Ref. 10 succeeded in dividing all their solutions of the time-dependent Hartree–Fock equations into three classes: periodic, quasiperiodic, and stochastic. To classify the solutions, they analyzed the multipole moments of the nuclear density:

$$M_{LI}(t) = \int d\mathbf{r} r^L Y_{LM}(\hat{r})\, \rho_I(\mathbf{r}, t), \tag{10}$$

where

$$p_I(\mathbf{r}, t) = \begin{cases} \rho_p(\mathbf{r}, t) + \rho_n(\mathbf{r}, t), & I = 0; \\ \rho_p(\mathbf{r}, t) - \rho_n(\mathbf{r}, t), & I = 1. \end{cases} \tag{11}$$

The anticorrelation function

$$C_{LI}(t) = \int_{-\infty}^{\infty} \frac{d\omega}{2\pi} e^{i\omega t} \mid M_{LI}(\omega) \mid^2 \tag{12}$$

is rapidly damped for the isoscalar quadrupole mode ($L = 2$, $I = 0$), so that the collective motion described by this mode can be classified as stochastic.

Chaotic dynamics, which represents one of the most general forms of evolution of a nonlinear system, is realized only in definite regions of the parameter values. This circumstance makes it necessary to answer the following questions:

1. Can one observe dynamical chaos in processes characteristic of collective nuclear dynamics?

2. If it is possible, at what critical energy does the transition from regular to random motion occur?

3. What features of stochastic dynamics are manifested at energies above the critical value?

In this review we attempt to find at least partial answers to these questions.

THE CRITERION OF NEGATIVE CURVATURE

Understanding by stochastization the appearance in a system of statistical properties due to local instability, we acquire the attractive possibility of identifying the parameter values at which local instability arises in the system with the transition to chaos. Unfortunately, the situation is in reality more complicated; for all existing criteria of stochasticity based on investigation of local instability have a well-known[11] shortcoming—loss of stability of regular motion does not necessarily lead to chaos. Instead, a transition to a different and more complicated type of regular motion is, in general, possible. Moreover, the very assertion that local instabilities determine the global dynamics of the system is controversial. Objections are also brought against individual details in the derivations of specific criteria of stochasticity. Despite these serious limitations, present experience[1-4] permits the conclusion that criteria of this kind give an important indication of transition from ordered to chaotic motion and in conjunction with numerical experiment greatly facilitate the analysis of multidimensional nonlinear motion.

Numerous criteria of stochasticity are based on direct estimation of the rate of separation of neighboring trajector-

ies in the phase space. We investigate[4] the behavior of two initially neighboring trajectories $\{\mathbf{q}_1(t), \mathbf{p}_1(t)\}$ and $\{\mathbf{q}_2(t), \mathbf{p}_2(t)\}$. The linearized equations of motion for the deviations

$$\xi(t) = \mathbf{q}_1(t) - \mathbf{q}_2(t); \ \eta(t) = \mathbf{p}_1(t) - \mathbf{p}_2(t) \tag{13}$$

have the form

$$\dot{\xi}(t) = \eta; \ \dot{\eta}(t) = -\hat{S}(t)\,\xi, \tag{14}$$

where $\hat{S}(t)$ is the matrix constructed from the second derivatives of the potential $V(\mathbf{q})$, calculated along the fiducial trajectory $\mathbf{q}_1(t)$:

$$S_{ij}(t) = \frac{\partial^2 V}{\partial q_i\,\partial q_j}\Big|_{\mathbf{q}=\mathbf{q}_1(t)}. \tag{15}$$

The stability of the motion of the dynamical system described by the Hamiltonian

$$H(\mathbf{p}, \mathbf{q}) = p^2/2 + V(\mathbf{q}), \tag{16}$$

is determined in the N-dimensional case by the $2N \times 2N$ matrix

$$\hat{\Gamma} = \begin{vmatrix} \hat{0} & \hat{I} \\ -\hat{S}(t) & 0 \end{vmatrix}, \tag{17}$$

where $\hat{0}$ and $\hat{I}$ are the zero and unit $N \times N$ matrices. One can find a time-dependent transformation T such that

$$(\hat{T}\Gamma(t)\,\hat{T}^{-1})_{ij} = \lambda_i(t)\,\delta_{ij}. \tag{18}$$

If at least one of the eigenvalues λ_i is real, then the separation of the trajectories grows exponentially, and the motion is unstable. Imaginary eigenvalues correspond to stable motion. In general, the eigenvalues and, therefore, the nature of the motion change with the time.

To diagonalize the matrix $\hat{\Gamma}(t)$, we must first solve the original equations of the motion, and this makes it difficult to carry out the task. The problem can be significantly simplified by assuming that the time dependence $\hat{S}(t)$ can be eliminated by replacement of the time-dependent point $\mathbf{q}_1(t)$ of the phase space by a time-independent coordinate q. This reduces Eqs. (14) for the variations to a system of autonomous linear differential equations:

$$\dot{\xi} = \eta; \ \dot{\eta} = -\hat{S}(q)\,\xi, \tag{19}$$

in which the coordinate $\mathbf{q}$ is regarded as a time-independent parameter. The problem of investigating the stability of the motion is then greatly simplified. Thus, for a system with two degrees of freedom the equation for the eigenvalues of the matrix Γ taken the form

$$\det \begin{vmatrix} -\lambda & 0 & 1 & 0 \\ 0 & -\lambda & 0 & 1 \\ -\frac{\partial^2 V}{\partial q_1^2} & -\frac{\partial^2 V}{\partial q_1\,\partial q_2} & -\lambda & 0 \\ -\frac{\partial^2 V}{\partial q_1\,\partial q_2} & -\frac{\partial^2 V}{\partial q_2^2} & 0 & -\lambda \end{vmatrix}. \tag{20}$$

Its solution is

$$\lambda_{1,2,3,4} = \pm\left[-b \pm \sqrt{b^2 - 4c}\right]^{1/2}, \tag{21}$$

where

$$\left.\begin{aligned} b &= \operatorname{Sp}\hat{S}(q) = \frac{\partial^2 V}{\partial q_1^2} + \frac{\partial^2 V}{\partial q_2^2}; \\ c &= \det\hat{S}(q) = \frac{\partial^2 V}{\partial q_1^2}\,\frac{\partial^2 V}{\partial q_2^2} - \left(\frac{\partial^2 V}{\partial q_1\,\partial q_2}\right)^2. \end{aligned}\right\} \tag{22}$$

We shall assume that $b > 0$. Then under the condition that $c > 0$ the solutions λ are purely imaginary and the motion is stable. For $c < 0$, the pair of roots becomes real, and this leads to exponential separation of neighboring trajectories, i.e., to instability of the motion. The determinant c has the same sign as the Gaussian curvature $K(q_1, q_2)$ of the potential-energy surface:

$$K(q_1, q_2) = \frac{\frac{\partial^2 V}{\partial q_1^2}\,\frac{\partial^2 V}{\partial q_2^2} - \left(\frac{\partial^2 V}{\partial q_1\,\partial q_2}\right)^2}{\left[1 + \left(\frac{\partial V}{\partial q_1}\right)^2 + \left(\frac{\partial V}{\partial q_2}\right)^2\right]^2}. \tag{23}$$

This association suggests[12] the possible existence of the following scenario for the transition from regular to random motion based on investigation of the Gaussian curvature of the potential-energy surface.

At low energies, motion near the minimum of the potential energy, where the curvature is certainly positive, is periodic or quasiperiodic in nature and is separated from the region of instability by a line of zero curvature. If the energy is increased, the "particle" will for a time be in the region of negative curvature of the potential-energy surface, where initially neighboring trajectories separate exponentially, and at large times this will ultimately lead to a motion that mimics random behavior and is usually called stochastic. In accordance with this scenario of stochastization, the critical energy of the transition to chaos is equal to the minimal value of the energy on the line of zero Gaussian curvature.

We now investigate the influence of the curvature of the potential-energy surface on the dynamics of a Hamiltonian system,[13] taking as an example the three-parameter family of potentials

$$V(x, y; A, B, \mu) = x^2 y + \frac{1}{3}\mu y^3 + \frac{1}{2}(Ax^2 + By^2). \tag{24}$$

We restrict ourselves to the case $A > 0$, $B > 0$, which ensures the existence of a minimum of the potential energy at the origin. For the parameter values $A = B = 1$, $\mu = -1$ the potential (24) reduces to the well-known Hénon–Heiles potential,[14] which has become the traditional testing ground for new ideas and methods associated with the investigation of stochastization in Hamiltonian systems. In connection with the problem of integrability another set of parameters, $A = B = \mu = 1$, which leads to the so-called modified Henon–Heiles potential, has also become very well known.

The Gaussian curvature of the considered potential-energy surface vanishes at the points that satisfy the equation

$$-\mu^{-1}x^2 + (y - y_0)^2 = R_0, \tag{25}$$

where

$$y_0 = -\frac{1}{4}\frac{B}{\mu}(1 - \varkappa); \ R_0 = -\frac{1}{4}\frac{B}{\mu}(1 + \varkappa); \ \varkappa = -\frac{A}{B}\mu. \tag{26}$$

For $\mu < 0$ the line of zero curvature of the potential (24) is an ellipse that for the Hénon–Heiles potential degenerates into a circle (Fig. 1a):

$$x^2 + y^2 = 1/4. \tag{27}$$

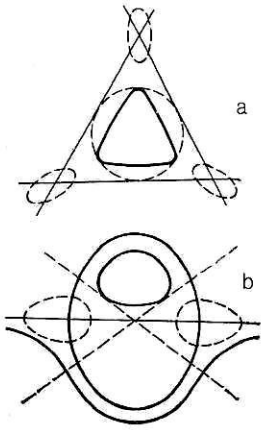

FIG. 1. Contours of the Hénon–Heiles potential (a) and the modified Hénon–Heiles potential (b). The broken lines and curves are the lines of zero Gaussian curvature.

In the case $\mu > 0$ the zero-curvature line is represented by the branches of a hyperbola, these degenerating for the modified Hénon–Heiles potential into two straight lines (Fig. 1b):

$$y = \pm x - 1/2. \tag{28}$$

For the potential (24) the energy on the zero-curvature line is determined by the expression

$$V(y;\ K=0) = \frac{3}{4}\mu y^3 + B(1-\varkappa)y^2 + \frac{1}{4}AB(2-\varkappa)y + \frac{1}{8}A^2B. \tag{29}$$

We consider in more detail the situation when the zero-curvature line is a closed curve ($\mu < 0$). Then within the interval $]y - R_0, y + R_0[$ the function $V(y;K=0)$ attains its greatest value at the point $\bar{y} = 1/4(B/\mu)\varkappa$. For $\varkappa < 1$ the value of the energy

$$V(\bar{y},\ K=0) = \frac{1}{48}\frac{B^3}{\mu^2}\varkappa^2(\varkappa+3) \tag{30}$$

is equal to the minimal energy $V_{\min}(K=0)$ on the zero-curvature line and, in accordance with the scenario of stochastization that we are considering, is the critical energy at which the transition from the stable regular motion to the unstable chaotic motion occurs. For $\varkappa > 1$, the minimal value of the energy on the zero-curvature line is attained at the edge of the interval, at one of the points $y_0 \pm R$, and

$$V_{\min}(K=0) = \frac{1}{12}\frac{B^3}{\mu^2}. \tag{31}$$

In particular, for the Hénon–Heiles potential ($\varkappa = 1$).

$$V_{\min}(K=0) = \frac{1}{48}\frac{B^3}{\mu^2}\varkappa^2(\varkappa+3) = \frac{1}{12}\frac{B^3}{\mu^2} = \frac{1}{12}. \tag{32}$$

In the case $\mu > 0$ (the branches of the hyperbola form the zero-curvature line), the minimal value of the energy is always attained at the point $\bar{y} = 1/4(B/\mu)\varkappa$. In particular, for the modified Hénon–Heiles potential ($\varkappa = -1$).

$$V_{\min}(K=0) = \frac{1}{48}\frac{B^3}{\mu^2}\varkappa^2(\varkappa+3) = \frac{1}{24}. \tag{33}$$

The values predicted above for the critical energy of the transition to chaos agree well with the results of numerical solution of the corresponding equations of motion. For the numerical investigation of nonliner Hamiltonian systems two main methods are traditionally used: the method of Poincaré maps and study of the rate of separation of neighboring trajectories. The method of Poincaré maps is particularly effective for systems with two degrees of freedom and a phase space of four dimensions. Because the energy is conserved, the trajectory of the "particle" lies on the three-dimensional surface $H(x,\dot{x},y,\dot{y}) = E$. Eliminating one of the variables, for example, $\dot{x}$, we consider the points of intersection of the phase trajectory with the plane $x = \text{const}$ ($x = 0$). In the general case they will be randomly distributed over some part of the $(y,\dot{y})$ plane bounded by a separatrix. If in addition to the energy there is a further integral of the motion $I(y,\dot{y}) = \text{const}$, then the successive crossings of the trajectory will lie in our chosen plane on some curve $y = f(\dot{y})$. Therefore, analysis of the Poincaré maps can establish the existence of additional integrals of the motion and, therefore, establish which type of motion is realized in the system for given values of its parameters in a definite region of the phase space.

Figure 2 shows the Poincaré maps (plots) for the Hénon–Heiles potential and the modified Hénon–Heiles potential at the saddle energy. Their striking difference—dynamic chaos in the first case and quasiperiodic motion in the second—is due to the following circumstance. As is well known, systems with two degrees of freedom are integrable only in exceptional cases. In particular, various approaches[3] give for the Hamiltonian

$$H = \frac{1}{2}(\dot{x}^2 + \dot{y}^2) + V(x,\ y;\ A,\ B,\ \mu), \tag{34}$$

where $V(x,y,A,B,\mu)$ is determined by the expression (24), the following conditions for integrability:

1) $\mu = 1$, $A = B$,
2) $\mu = 6$, A and B arbitrary;
3) $\mu = 16$, $B = 16A$.

Condition 1 exactly corresponds to the modified Hénon–Heiles potential, which by the simple substitution $x = u + v$, $y = u - v$ reduces to a separable and, therefore, integrable potential. However, even a small perturbation of the parameters of the potential, leading to the nonintegrable situation, enables us to observe chaos in the modified Hénon–Heiles potential as well. Figure 3 shows the Poincaré maps for distorted ($A/B = 0.8$) Hénon–Heiles and modified Hénon–Heiles potentials. Figure 3a does not differ qualitatively from the unperturbed case (Fig. 2a), but the Poincaré map

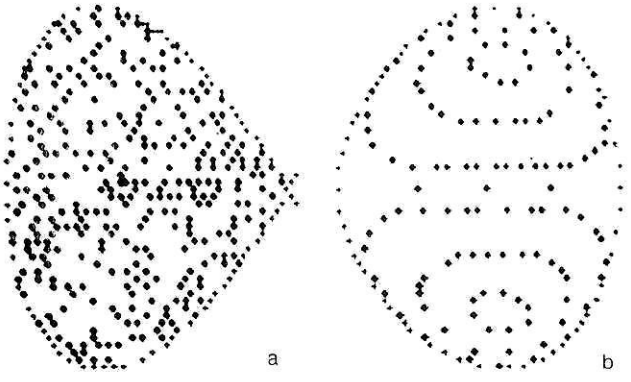

FIG. 2. Poincaré maps for the Hénon–Heiles potential (a) and the modified Hénon–Heiles potential (b) at the dissociation energy.

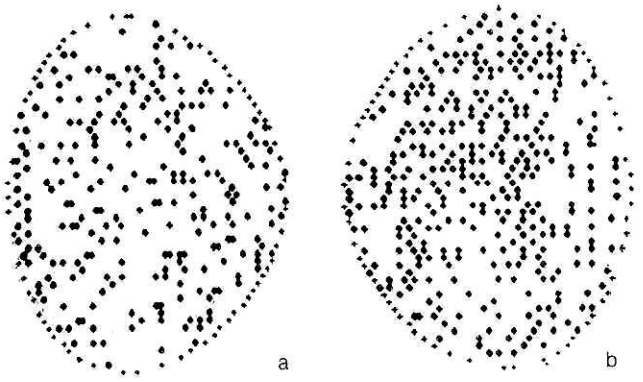

FIG. 3. Poincaré maps for the distorted ($A/B = 0.8$) Hénon–Heiles potential (a) and the modified Hénon–Heiles potential (b).

of the perturbed modified Hénon–Heiles potential contains all the characteristic features of stochastic motion.

Poincaré maps permit a perspicuous representation of the phase-space topology. However, to estimate the extent of the disorder, it is convenient to use the circumstance that the separation between initially neighboring points that lie in the chaotic region of the phase space increases exponentially as a function of the time, whereas in the case of ordered motion there is only linear growth. We define[15] a measure of local separation of the trajectories:

$$k_n(t,\ z_0,\ d_0) = \frac{1}{n}\sum_{i=1}^{n} \ln \frac{|d_i|}{|d_0|}, \tag{35}$$

where d_0 and d_i are the separations in the phase space between the trajectories at the times $t = 0(d_0)$ and $t_i = t/n(d_i)$, and n is the number of divisions of the trajectories. It follows from numerical calculations that if d_0 is not too large, then:

1) $\lim_{n\to\infty} k_n(t,z_0,d_0) = k(t,z_0,d_0)$ exists;
2) $k(t,z_0,d_0)$ does not depend on t;
3) $k(t,z_0,d_0)$ does not depend on d_0;
4) $k(t,z_0,d_0) = 0$ if z_0 is chosen in a regular region of the phase space;
5) $k(t,z_0,d_0)$ does not depend on the choice of z_0 if z_0 is chosen in the chaotic region of the phase space, and in this case

$$k(t,\ z_0,\ d_0) > 0. \tag{36}$$

Properties 2, 3, and 5 make it possible to speak of $k(E)$ instead of $k(t,z_0,d_0)$ when z_0 belongs to the chaotic region of the phase space. Properties 1–3 can be explained[16] on the basis of the connection between $k(t,z_0,d_0)$ and the Lyapunov characteristic exponents, but at the present time properties 4 and 5 must be regarded as empirical. Nevertheless, the construction (35) is not only a natural parameter that determines the degree of development of stochasticity in the system and one convenient for numerical calculations but is also intimately related to the so-called dynamical entropy,[17] which represents the rate of change of the coarse-grained entropy of a Hamiltonian system.

To prove the existence of a correlation between the measure k_n of the local separation of trajectories and the Gaussian curvature of the potential-energy surface, we investigate

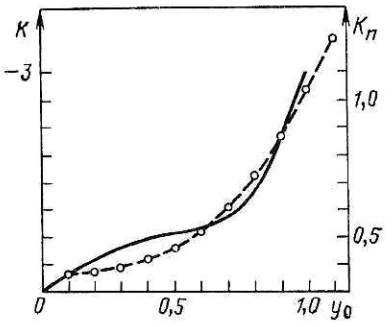

FIG. 4. Dependence of the Gaussian curvature K (continuous curve) and measure of the local separation of trajectories k_n (broken curve) on the choice of the initial conditions ($x = 0$).

the dependence of this quantity on the choice of the initial conditions. Figure 4 shows such a dependence for the Hénon–Heiles potential. The initial points were chosen on the y axis; the region $0 < y < \frac{1}{2}$ corresponds to positive values of the Gaussian curvature K, while in the region $\frac{1}{2} < y < 1$ the Gaussian curvature becomes negative and reaches the value $K = -3$ at the saddle point at $y = 1$. With increasing Gaussian curvature the parameter k_n also increases. In the numerical calculations values of d_0 in the interval 0.01–0.001, with $t \sim 1$, were used.

To describe the dynamics of the system for energies exceeding the critical value, it is necessary to study the dependence of k_n on the energy at large times. In this case, k_n ceases to depend on the initial conditions if they are chosen in the chaotic region, and, as we have already noted, it is a convenient measure of the extent of chaos in the system. The trajectory calculations over large time intervals necessary for this purpose can be avoided by using the ergodicity of the chaotic component of the motion. We calculated k_n over very short time intervals ($T \sim 5t$), but with averaging over the phase space (about 1000 initial values). The results, given in Fig. 5, were, as expected, close to the data of Ref. 15 corresponding to trajectory calculations for times $T \sim (10^4$–$10^5)t$. This dependence of k_n on the energy reflects the well-known growth of stochasticity in the Hénon–Heiles potential obtained from analysis of the Poincaré sections.[14]

Using this method to determine the measure k_n of local separation, we were able to investigate the nature of the motion in the potential (24) for variation of its parameters in

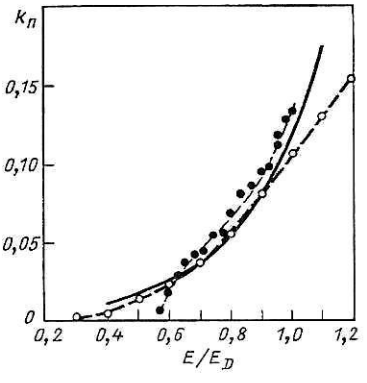

FIG. 5. Energy dependence of k_n for different methods of averaging: with respect to the time (black circles, data of Ref. 15) and with respect to the initial values (open circles). The continuous curve corresponds to the exponential dependence that approximates k_n in accordance with the data of Ref. 15; E_D is the dissociation energy.

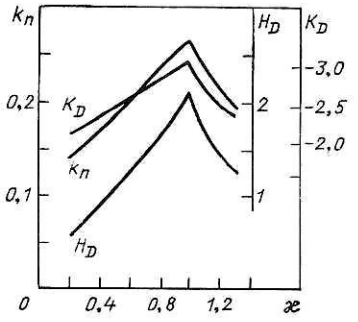

FIG. 6. Dependence of the measure of local separation, k_n, the Gaussian curvature, K_D, and the mean curvature, H_D, at the saddle points on the parameter $\varkappa$. The energy is equal to the dissociation energy.

wide ranges. Figure 6 gives k_n at the saddle energy as a function of the parameter $\varkappa = (A/B)\mu$ and also the Gaussian curvature K_s and mean curvature $H_s = \mathrm{Sp}\,\hat{S}(\mathbf{q})$ as functions of the same parameter. It can be clearly seen that a deviation of the parameter from unity leads to a decrease of the measure of dynamical chaos in the system and that this decrease is clearly correlated with the decrease of the curvature at the saddle points.

Thus, numerical calculations of the dynamics in the considered family of nonlinear potentials confirms the part played by the curvature of the potential-energy surface in the occurrence of the instability that leads to the transition from regular to chaotic motion.

DYNAMICS OF FINITE MOTION IN POTENTIALS WITH SEVERAL LOCAL MINIMA

The example just considered—the dynamics of the system described by the generalized Hénon–Heiles potential—supports the idea that the criterion of negative curvature gives an important indication of the transition from regular to chaotic motion. Its use for numerous Hamiltonian systems led to promising results.[18] The interpretation of negative curvature of the potential-energy surface as the source of local instability permits well-known grounded prediction of the existence of chaotic regimes in a studied system and also estimation of the region of energies in which the transition to these regimes occurs. The effectiveness of the approach based on analysis of the potential-energy surface is enhanced by its generality, which permits its application to a large class of nonlinear Hamiltonian systems irrespective of their particular nature.

Although in numerous cases the negative-curvature criterion correctly predicts the critical energy of the transition to chaos, we must not forget that we are dealing here, not with a rigorous criterion, but only with a weak indicator of loss of stability of a certain type of regular motion, and that this loss need not, in general, lead to chaos. In part, the limitation of the criterion is due to the assumptions made in its justification, the key step being the transition from the nonautonomous equations (14) to the autonomous equations (19) by replacement of a coordinate that lies on the fiducial trajectory by an arbitrary phase coordinate. Such a procedure can be justified only over a sufficiently short time interval, during which the matrix $\hat{\Gamma}$ can be regarded as approximately constant. In this sense our stability analysis has a rigorously local nature and leaves open the question of the connection between local instability and the global behavior of the system.

The complexity of the situation is well illustrated by the dynamics of finite motion in potentials with several local minima. A Hamiltonian system with a potential-energy surface possessing several local minima provides a fairly simple model in the framework of which one can describe the main features of the dynamics of the transition between different equilibrium states, inciuding important transitions such as chemical reactions, nuclear fission, etc. Being richer than in the case of potentials with a single minimum, the geometry of such a potential-energy surface permits the existence of several critical energies even for a fixed set of parameters of the potential. This circumstance leads to the existence, for such potentials, of mixed states, i.e., at the same energy different dynamical regimes are realized in different minima.

The specific features of the problem can be demonstrated by the example of the Hamiltonian

$$H = \frac{1}{2}(\dot{x}^2 + \dot{y}^2) + \frac{1}{4}y^4 + x^2y + ax^2 - y^2. \tag{37}$$

The mass parameters for the two independent directions have been taken to be equal, since the discovery of stochasticity for equal mass parameters guarantees its existence as well for the case when they are different.

The geometry of the two-dimensional single-parameter potential

$$V(x,\ y;\ a) = \frac{1}{4}y^4 + x^2y + ax^2 - y^2 \tag{38}$$

is determined by five (for $a > \sqrt{2}$) critical points: two minima of equal depth, the first of which, with coordinates $x = 0$, $y = -\sqrt{2}$, we shall in what follows call the left well and the second, with coordinates $x = 0$, $y = \sqrt{2}$, the right well, and three saddles with coordinates $x = \pm\sqrt{a^3 - 2a}$, $y = -a$, and $x = 0$, $y = 0$. The parameter a determines the potential energy at the side saddles:

$$V(x = \pm\sqrt{a^3 - 2a},\ y = -a) = \frac{1}{4}\ a^4 - a^2. \tag{39}$$

The energy of the saddle at the origin does not depend on a and is equal to zero. Therefore, for negative energies the motion will be localized in an individual well. For $a = 2$ (this case will be investigated in the most detail) the energies at all the saddles are equal.

We now estimate the critical energy of the transition to chaos using the negative-curvature criterion. In this case, the problem reduces to finding a conditional extremum—the minimum of the potential energy on the zero-curvature line. This line is described by the equation

$$(y + a)(3y^2 - 2) - 2x^2 = 0. \tag{40}$$

For $a = 2$, we arrive at a value of the critical energy that is the same for the two wells and is equal to

$$E_{cr} = V_{\min}\ (K = 0) = -5/9. \tag{41}$$

We now turn to an analysis of numerical solutions of the equations of motion generated by the Hamiltonian (38). Figure 7 gives Poincaré maps for different energies ($a = 2$) that demonstrate the transition from regular to chaotic motion for the two minima. The motion represented in Fig. 7a has a clearly expressed quasiperiodic nature for both the left and the right well. Note the difference in the structure of the Poincaré maps for the different minima, namely, the complicated structure with several fixed points at the left minimum

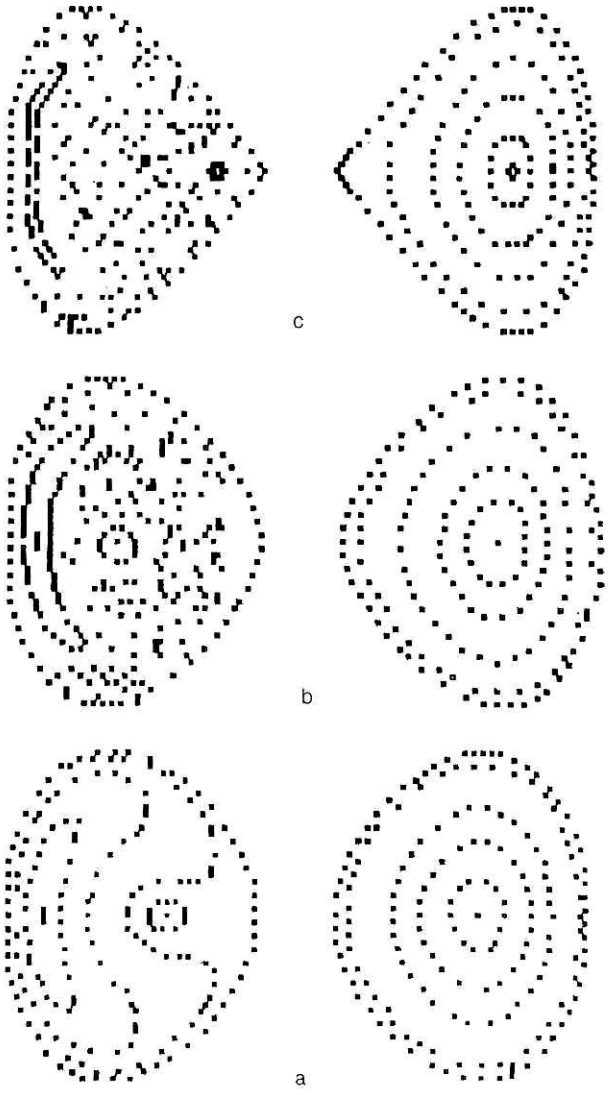

FIG. 7. Poincaré maps for the potential (37) at different energies: a) $E = -0.9$; b) $E = -0.5$; c) $E = 0$.

and the simple structure with a single fixed point at the right minimum. As the energy is raised, we observe a gradual transition to chaos, but the change in the nature of the motion of the trajectories localized in a particular minimum is very different. Whereas for the left well an increase of the energy to about half the saddle energy (Fig. 7b) results in a gradual transition to chaos and its increase to the saddle energy (Fig. 7c) has the consequence that practically all initial conditions lead to chaotic trajectories, the motion at the same energies in the second minimum remains quasiperiodic. Moreover, even at an energy appreciably exceeding the saddle energy there still remains in the right well an appreciable fraction of the phase space that corresponds to quasiperiodic motion.

Analysis of the Poincaré maps permits the introduction of a critical energy of transition to chaos, this being defined as the energy at which the proportion of the phase space with random motion exceeds some arbitrarily chosen value. The indefiniteness is due to the absence of a sharp transition to chaos for any critical value of the perturbation to which an integrable problem is subjected. Therefore, when an "approximate" critical energy obtained by numerical modeling is compared with a "critical" value obtained by means of analytic estimates, i.e., on the basis of various criteria of stochasticity, a certain care must be exercised. Figure 8 shows the measure of the growth of chaos in the left well as a function of the energy as obtained by means of analysis of the Poincaré maps. The arrow indicates the value of the critical energy found from the negative-curvature criterion. At this energy the stochastic component of the motion reaches about 10% of the accessible phase space.

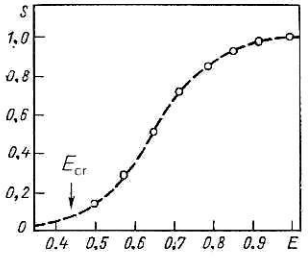

FIG. 8. Measure of the growth of chaos in the left well as a function of the energy (S is the fraction of initial conditions that generate chaotic trajectories).

Thus, the critical energy determined by the negative-curvature criterion for the left well agrees well with the critical energy obtained by numerical modeling but contradicts it for the right well, where the numerical modeling reveals the appearance of chaos only when the saddle energy has been reached. This contradiction forces us to resort to stochasticity criteria based on the theory of nonlinear resonance in multidimensional systems.

One of the first widely used criteria for the transition to chaos is the so-called criterion of overlapping of nonlinear resonances.[19] According to this criterion, the occurrence of local instability in a Hamiltonian system is due to the touching of the separatrices of individual nonlinear resonances. The scenario of the transition to chaos based on the overlapping of resonances is as follows.[20] The averaged motion of a system in the neighborhood of an isolated nonlinear resonance in the plane of the action–angle variables is similar to the behavior of a particle in a potential well. To some resonances there correspond several potential wells. Overlapping of the resonances means that the potential wells approach each other in such a way that a random walk of the particle between them becomes possible.

This approach must be somewhat modified for systems that are described by a Hamiltonian with a single resonance term. In this case, the occurrence of large-scale stochasticity is due[21] to the breakup of the stochastic layer near the separatrix of the unique resonance. The essence of the modification consists in the approximate reduction, in the neighborhood of the resonance, of the original Hamiltonian to the Hamiltonian of a nonlinear pendulum interacting with a periodic perturbation:

$$H(v,\ x,\ \tau) = \frac{1}{2}v^2 - M\cos x - P\cos k(x-\tau). \qquad (42)$$

The width w of the stochastic layer of the resonance is[22]

$$w \sim \rho e^{-1/\rho}/M\rho^{2k+1}, \qquad (43)$$

where

$$\rho = 2M^{1/2}/\pi k. \qquad (44)$$

If P/M has the order ρ^s, then

$$w \sim \rho^{-\lambda} e^{-1/\rho}, \tag{45}$$

where

$$\lambda = 2k + 1 - s. \tag{46}$$

For

$$\rho_i = \frac{1}{\lambda}[1 - (1+\lambda)^{-1/2}] \tag{47}$$

the function $w(\rho)$ has a point of inflection. The rapid growth of w makes it possible to determine the threshold of the breakup of the stochastic layer as the value

$$\rho_s = \lambda^{-2}[(1+\lambda)^{1/2} - 1]^2 \tag{48}$$

of ρ at which the tangent to the point ρ_i of the function w intersects the ρ axis.

We use this method to find the threshold of the transition to large-scale stochasticity of the system described by the Hamiltonian (37). This Hamiltonian in coordinate systems with origins at the left well (upper sign) and right well (lower sign) has the form

$$H = \frac{1}{2}(\dot{x}^2 + \omega_1^2 x^2) + \frac{1}{2}(\dot{y}^2 + \omega_2^2 y^2) + x^2 y \mp \sqrt{2}\, y^3 + \frac{1}{4} y^4, \tag{49}$$

where

$$\omega_1 = [2(a \mp \sqrt{2})]^{1/2}, \quad \omega_2 = 2. \tag{50}$$

For $a = 2$,

$$\omega_1 \simeq \begin{cases} 1{,}0824, \\ 2{,}6131. \end{cases} \tag{51}$$

We make a canonical transformation to action–angle variables:

$$\left.\begin{aligned} x &= \left(\frac{2\mathcal{J}_1}{\omega_1}\right)^{1/2} \cos\varphi_1, \quad y = \left(\frac{2\mathcal{J}_2}{\omega_2}\right)^{1/2} \cos\varphi_2; \\ \dot{x} &= (2\mathcal{J}_1\omega_1)^{1/2} \sin\varphi_1, \quad \dot{y} = (2\mathcal{J}_2\omega_2)^{1/2} \sin\varphi_2. \end{aligned}\right\} \tag{52}$$

In these variables, the Hamiltonian (49) becomes

$$\begin{aligned} H(\mathcal{J}_1, \mathcal{J}_2; \varphi_1, \varphi_2) &= H_0(\mathcal{J}_1, \mathcal{J}_2) \\ &+ \sum_{m_1,\, m_2 \in \mathcal{Y}} f_{m_1 m_2}(\mathcal{J}_1\mathcal{J}_2)\cos(m_1\varphi_1 + m_2\varphi_2); \end{aligned} \tag{53}$$

$$\mathcal{Y}: [0,\ 1],\ [0,\ 2],\ [0,\ 3],\ [0,\ 4],\ [2,\ 1],\ [2,\ -1],$$

where

$$\left.\begin{aligned} H_0(\mathcal{J}_1, \mathcal{J}_2) &= \mathcal{J}_1\omega_1 + \mathcal{J}_2\omega_2 + \frac{3}{8}\frac{\mathcal{J}_2^2}{\omega_2^2} - 1; \\ f_{01} &= \frac{\mathcal{J}_1}{\omega_1}\left(\frac{2\mathcal{J}_2}{\omega_2}\right)^{1/2} \pm 3\left(\frac{\mathcal{J}_2}{\omega_2}\right)^{3/2}; \\ f_{02} &= \frac{1}{2}\frac{\mathcal{J}_2^2}{\omega_2^2}, \quad f_{03} = \pm\left(\frac{\mathcal{J}_2}{\omega_2}\right)^{3/2}; \\ f_{04} &= \frac{1}{8}\frac{\mathcal{J}_2^2}{\omega_2^2}; \quad f_{21} = f_{2,-1} = \frac{1}{2}\frac{\mathcal{J}_1}{\omega_1}\left(\frac{2\mathcal{J}_2}{\omega_2}\right)^{1/2}. \end{aligned}\right\} \tag{54}$$

The term with indices $\mathbf{r} = (r_1, r_2)$ is called a resonance term for the given value E of the energy if there exist action variables $(\mathcal{J}_1^r, \mathcal{J}_2^r)$ such that $E = H_0(\mathcal{J}_1^r, \mathcal{J}_2^r)$ and

$$r_2\bar{\omega}_1(\mathcal{J}_1^r, \mathcal{J}_2^r) + r_2\bar{\omega}_2(\mathcal{J}_1^r, \mathcal{J}_2^r) = 0, \tag{55}$$

where

$$\bar{\omega}_i = \partial H_0/\partial\mathcal{J}_i \ (i = 1,\ 2). \tag{56}$$

If at energies corresponding to finite motion $(-1 < E < 0)$ we are sufficiently far from the resonance, i.e., for all (m_1, m_2)

$$|m_1\bar{\omega}_1 + m_2\bar{\omega}_2| \gg f_{m_1 m_2}, \tag{57}$$

then we can, avoiding the problem of "small denominators," make a canonical transformation to new action–angle variables that eliminate the angular dependence in the lowest order in the small parameter identified with the energy. The result of this procedure is a redefinition of the integrable part $H_0(\mathcal{J}_1, \mathcal{J}_2)$ of the original Hamiltonian and an extension of the set $\mathcal{Y}$ of terms that depend on the angles. One of the following three cases is then obtained:

1) as before, there are no resonance terms in the region of energies in which we are interested;

2) a single resonance term arises;

3) several resonance terms arise.

In the first case we make a new canonical transformation and continue this procedure until we encounter situations 2 or 3. In the second case the critical energy at which the transition to large-scale stochasticity occurs can be determined by the method of the breakup of the stochastic layer,[21] whereas to find the critical energy in the third case one can use the criterion of overlapping of resonances.[19]

Near the resonance a small mismatch,

$$|m_1\bar{\omega}_1 + m_2\bar{\omega}_2| \leqslant f_{m_1 m_2}, \tag{58}$$

can be compensated by terms of higher order obtained by means of a further canonical transformation of the nonresonance terms. In the case $a = 2$ the condition (58) of a weak mismatch is satisfied for the resonance $(2, -1)$, and the procedure outlined above leads to the expression

$$\begin{aligned} H_0 = \mathcal{J}_1\omega_1 + \mathcal{J}_2\omega_2 - 1 + \frac{3}{8}\frac{\mathcal{J}_2^2}{\omega_2^2} - \frac{4\omega_1 + 5}{32\omega_1^2(\omega_1+1)}\mathcal{J}_1^2 \\ + \left[\pm\frac{3\sqrt{2}}{2} - \frac{1}{\omega_1(\omega_1+1)}\right]\frac{\mathcal{J}_1\mathcal{J}_2}{8\omega_1}. \end{aligned} \tag{59}$$

In the left well we retain from the angle-dependent terms only two: the resonance term

$$\frac{1}{2}\frac{\mathcal{J}_1}{\omega_1}\left(\frac{2\mathcal{J}_2}{\omega_2}\right)^{1/2}\cos(2\varphi_1 - \varphi_2) \tag{60}$$

and the "pumping" term[21]

$$\frac{\sqrt{2}}{64\omega_1}\left[\frac{3}{\omega_1+1} + \frac{1}{\omega_1}\right]\mathcal{J}_1\mathcal{J}_2\cos(2\varphi_1 - 2\varphi_2), \tag{61}$$

the direction $\mathbf{m}$ of which is the closest to the resonance $\mathbf{r}$. After this, direct application of the criterion of breakup of the stochastic layer leads to the value of the critical energy in the left well:

$$E_{cr} \simeq -0.51, \tag{62}$$

which agrees well with the result of the numerical solution of the equations of motion. Direct analysis of the integrable part of the Hamiltonian (59) shows that in the right well there are no resonances, so that, in complete accordance with the numerical results, the transition to large-scale stochasticity is possible only when the saddle energy is reached.

POTENTIALS OF THE LOW UMBILIC CATASTROPHES AND BIRKHOFF–GUSTAVSON NORMAL FORMS

The mixed state demonstrated in the previous section is typical for a large class of two-dimensional potentials with

Table I. Potentials of umbilic catastrophes.

Potential	Germ	Perturbation	Conditions M^*	Topology	E_M	E_D	E_{cr}
D_4^-	$x^2y-\frac{1}{3}y^3$	ay^2-by	$b=\frac{3}{4}a^2$	$a=1$ $b=3/4$ 	$-\frac{1}{6}$	0	$-\frac{1}{12}$
D_5	$x^2y+\frac{1}{4}y^4$	ax^2-by^2	$b=\frac{1}{4}a^2$	$a=2$ $b=1$ 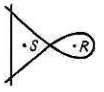	-1	0	$-\frac{5}{9}$
D_6^-	$x^2y-\frac{1}{5}y^5$	$ay^3-by+cx^2$	$b=a^2$ $c=2a$	$a=1$ $b=1$ $c=2$ 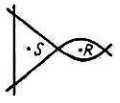	$-\frac{2}{5}$	$\frac{2}{5}$	$-0,06$
D_7	$x^2y+\frac{1}{6}y^6$	$ay^4+by^2+cx^2$	$b=\frac{3}{2}a^2$ $c=2\sqrt{a}$	$a=1/2$ $b=3/8$ $c=\sqrt{2}$ 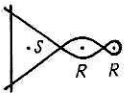	0	$\frac{1}{12}$	0,034

*The energies of all saddle points are equal to E_D, and the energies of all minima to E_M.

Note. If the conditions of Maxwell[23] are satisfied, the energies of all saddle points are equal to E_D, and the energies of all minima to E_M. The symbol R identifies minima at which chaos commences only when the saddle energy is reached; the symbol S, minima for which the critical energy can be determined by the negative-curvature criterion.

several local minima. We have restricted ourselves to the investigation of potentials of degree not higher than the sixth and symmetric with respect to the $x = 0$ plane. However, even under such restrictions the possible set of potential forms, which depend, in general, on 12 parameters, is too large. To reduce the volume of work, but still remaining fairly general, one can use the methods of catastrophe theory.[23] According to it, a fairly large class of polynomial potentials with several local minima is encompassed by the germs of the lowest umbilic catastrophes of the type D_4^+, D_5, D_6^+, D_7 subjected to definite perturbations. Thus, the potential (24) of Hénon–Heiles type is identical, apart from linear perturbing terms, to the elliptic umbilic D_4^- (Ref. 23).

Table I gives the values of the critical energy for the lowest umbilics as determined by the method of Poincaré maps and the negative-curvature criterion. For all minima possessing a complicated structure of the Poincaré maps with several fixed points the critical energy obtained by the negative-curvature criterion is close to the one obtained by numerical solution of the equations of motion. For the minima that possess a unique elliptic fixed point, chaos is observed only when the saddle energy is reached. This observation permits use of the following method to determine the critical energy. Having studied the structure of the Poincaré maps at low energies in each of the local minima, one can imnediately identify those of them in which the critical energy can be determined by the negative-curvature criterion. In the remaining minima, the critical energy must be identified with the saddle energy. This method is much simpler than the use of criteria for the transition to chaos associated with some version of the overlapping of nonlinear resonances.

The topology of the Poincaré maps can be reproduced without recourse to nunerical solution of the equations of motion. For this we use the method of studying classical nonseparable systems proposed by Birkhoff.[24] If the Hamiltonian $H(\mathbf{p},\mathbf{q})$ can be represented in the form of a power series in which its quadratic terms are a sum of the Hamiltonians of uncoupled harmonic oscillators with incommensurable frequencies, then there exists a canonical transformation $(\mathbf{p},\mathbf{q}) \to (\boldsymbol{\xi},\boldsymbol{\eta})$ such that the Hamiltonian in the new variables is a power series in $(\xi^2 + \eta^2)$. Gustavson[25] modified Birkhoff's method to the case of commensurable frequencies. When the Hamiltonian obtained in this manner—the Birkhoff–Gustavson normal form—is truncated in an appropriate order in the nonlinearity parameter, it permits an integrable approximation to the original nonintegrable Hamiltonian.

We consider the procedure for transformation to normal form of a Hamiltonian that is a power series in the coordinates and momenta:

$$H(\mathbf{u}, \mathbf{V}) = H^2(\mathbf{u}, \mathbf{v}) + H^{(3)}(\mathbf{u}, \mathbf{v}) + \ldots, \tag{63}$$

where

$$H^{(s)}(\mathbf{u}, \mathbf{v}) = \sum_{|i|+|j|=s} a_{ij} u^i v^j, \quad s = 2, 3 \ldots; \tag{64}$$
$$u^i = u_1^{i_1} u_2^{i_2} \ldots u_N^{i_N}; \quad |i| = i_1 + i_2 + \ldots i_N.$$

For systems with a positive-definite Hamiltonian $H^{(2)}$ there exists a canonical transformation $(\mathbf{u},\mathbf{v}) \to (\mathbf{q},\mathbf{p})$ such that

$$H^2(\mathbf{q}, \mathbf{p}) = \sum_{k=1}^{N} \frac{1}{2} \omega_k (q_k^2 + p_k^2). \tag{65}$$

We shall say that the Hamiltonian $H(\mathbf{q},\mathbf{p})$ is represented in normal form if

$$DH(\mathbf{q}, \mathbf{p}) = 0, \tag{66}$$

where

$$D = -\sum_k \omega_k \left(q_k \frac{\partial}{\partial p_k} - p_k \frac{\partial}{\partial q_k} \right). \tag{67}$$

This condition is equivalent to the requirement of vanishing of the Poisson bracket of $H^{(2)}$ and H, since

$$D = -[H^{(2)}, \ldots]. \tag{68}$$

The procedure for reducing the Hamiltonian to normal form can be realized[26] by a succession of canonical transformations, each of which reduces to normal form the unnormalized term of lowest order. The generating function needed to implement an individual transformation is

$$F(\mathbf{Pq}) = \sum_k P_k q_k + W^{(s)}(\mathbf{P}, \mathbf{q}). \tag{69}$$

The connection between the old (p,q) and new (P,Q) variables is

$$Q_k = q_k + \frac{\partial W^{(s)}}{\partial P_k}, \quad p_k = P_k + \frac{\partial W^{(s)}}{\partial q_k}, \quad H(\mathbf{p}, \mathbf{q}) = \Gamma(\mathbf{P}, \mathbf{Q}), \tag{70}$$

where $\Gamma(\mathbf{P},\mathbf{Q})$ is the Hamiltonian in the new variables. Expanding the new and old Hamiltonians in Taylor series near the points $\mathbf{P}$ and $\mathbf{q}$, we arrive at an equation for the sth component W^s of the generating function:

$$DW^{(s)}(\mathbf{P}, \mathbf{q}) = \Gamma^{(s)}(\mathbf{P}, \mathbf{q}) - H^{(s)}(\mathbf{P}, \mathbf{q}). \tag{71}$$

To solve this equation, we go over to the variables $(\boldsymbol{\eta}, \boldsymbol{\xi})$:

$$P_k = \frac{1}{\sqrt{2}}(\eta_k + i\xi_k); \quad q_k = i\sqrt{2}(\eta_k - i\xi_k), \tag{72}$$

which diagonalize the operator D:

$$D \to \tilde{D}(\boldsymbol{\eta}, \boldsymbol{\xi}) = i \sum \omega_k \left(\xi_k \frac{\partial}{\partial \xi_k} - \eta_k \frac{\partial}{\partial \eta_k} \right). \tag{73}$$

The solution of Eq. (71) in the variables η and ξ has the form

$$\tilde{W}^{(s)} = \tilde{D}^{-1}(\tilde{\Gamma}^{(s)} - \tilde{H}^{(s)}). \tag{74}$$

Here, $\tilde{H}^{(s)}$ is a known function, and the function $\tilde{\Gamma}^{(s)}$ can be determined by requiring finiteness of $\tilde{W}^{(s)}$. Therefore, the function $\tilde{\Gamma}^{(s)}$ must be chosen in such a way that all the terms in $\tilde{H}^{(s)}$ that could lead to vanishing of the denominator in the expression (74) cancel exactly. Such terms are usually[25] called null-space terms. Separating in $\tilde{H}^{(s)}$ the null-space terms $\tilde{N}^{(s)}$, we represent the solution (74) in the form

$$\tilde{\Gamma}^{(s)} = \tilde{N}^{(s)}, \tag{75}$$

$$\tilde{W}^{(s)} = \tilde{D}^{-1}(\tilde{H}^{(s)} - \tilde{N}^{(s)}). \tag{76}$$

To make this solution unique, it is sufficient to require the absence of null-space components in the generating function.

As an example, we give the normal form (up to $s = 6$) for the Hamiltonian (37) with $a = 2$ near the right minimum:

$$H(\mathcal{J}_1, \mathcal{J}_2) = 2{,}6131\mathcal{J}_1 + 2\mathcal{J}_2 - 0{,}2194\mathcal{J}_1\mathcal{J}_2 - 0{,}0167\mathcal{J}_1^2 - 0{,}375\mathcal{J}_2^2 - 0{,}0015\mathcal{J}_1^3 - 0{,}0283\mathcal{J}_1^2\mathcal{J}_2 - 0{,}1222\mathcal{J}_1\mathcal{J}_2^2 - 0{,}1328\mathcal{J}_2^3. \tag{77}$$

Commensurability of the frequencies leads to an extension of the set of null-space terms. Indeed,

$$\tilde{D}\eta_1^{m_1}\xi_2^{m_2} = i(m_1\omega_1 - m_2\omega_2)\eta_1^{m_1}\xi_2^{m_2} \tag{78}$$

and under the additional condition

$$m_1\omega_1 - m_2\omega_2 = 0 \tag{79}$$

$\tilde{D}^{-1}\eta_1^{m_1}\eta_2^{m_2}$ diverges. To avoid this divergence, the function $\tilde{\Gamma}^{(s)}$ in the case of commensurable frequencies must be chosen in such a way that the additional terms in $\tilde{H}^{(s)}$ that lead to divergences cancel. Except for this one point, the procedure of reduction to normal form is identical to that of the case of incommensurable frequencies.

STOCHASTIC DYNAMICS OF QUADRUPOLE VIBRATIONS OF NUCLEI

The main subject of study in the traditional theory of collective nuclear excitations is that of the regular solutions of the corresponding equations of motion. Although allowance for nonlinear effects does significantly modify the collective spectra and excitation probabilities of the corresponding collective modes, it does not lead to a radical change in the nature of the motion. As we have seen above, interpretation of the nucleus as a nonlinear multidimensional Hamiltonian system permits under certain conditions a transition from regular to chaotic motion. In this section, we investigate this possibility for quadrupole surface vibrations of nuclei described by the the deformation potential[6]

$$U(a_0, a_2) = \frac{c_2}{2}(a_0^2 + 2a_2^2) + \sqrt{\frac{2}{35}} c_3 a_0 (6a_2^2 - a_0^2) + \frac{c_4}{4}(a_0^2 + 2a_2^2)^2, \tag{80}$$

where a_0 and a_2 are internal coordinates of the surface of the nucleus undergoing quadrupole vibrations,

$$R(\theta, \varphi) = R_0 \{1 + a_0 Y_{20}(\theta, \varphi) + a_2 [Y_{2,2}(\theta, \varphi) + Y_{2,-2}(\theta, \varphi)]\}, \tag{81}$$

while the constants c_2, c_3, and c_4 can be regarded as phenomenological parameters that can be related by means of adiabatic time-dependent Hartree–Fock theory to the effective interaction of the nucleons in the nucleus. The potential (80) represents the lowest terms of the expansion in the deformation parameters of the more general expression[27]

$$U(a_0, a_2) = \sum_{m,n} c_{mn}(a_0^2 + 2a_2^2)^m a_0^n (6a_2^2 - a_0^2)^n. \tag{82}$$

Since the construction of (82) used solely the transformation properties of the interaction and the symmetry of the vibrations, this same expression describes the energy of the quadrupole vibrations of a liquid drop of any nature, the specific properties of the drop being entirely expressed in the coefficients c_{mn}.

In place of the coordinates a_0 and a_2 one often uses the coordinates β and γ:

$$a_0 = \beta \cos\gamma; \quad a_2 = \frac{\sqrt{2}}{2}\beta \sin\gamma, \tag{83}$$

where β is the deformation parameter of an axisymmetric nucleus, and γ is the parameter of "nonaxiality." To investigate the topology of the potential, it is convenient to go over

to the coordinates

$$x = \sqrt{2}\, a_2 = \beta \sin\gamma; \quad y = a_0 = \beta\cos\gamma, \tag{84}$$

in which the potential (80) takes the form

$$U(x,\ y;\ a,\ b,\ c) = \frac{a}{2}(x^2+y^2) + b\left(x^2y - \frac{1}{3}y^3\right) + c(x^2+y^2)^2, \tag{85}$$

$$a = c_2,\ b = 3\sqrt{\frac{2}{35}}c_3,\ c = \frac{1}{5}c_4$$

or

$$U(\beta,\ \gamma;\ a,\ b,\ c) = \frac{1}{2}a\beta^2 - \frac{1}{3}b\beta^3\cos 3\gamma + c\beta^4. \tag{86}$$

The parameters c_2, c_3, c_4 (a,b,c) have been estimated in various phenomenological models.[28] They vary in such wide ranges that it is sensible to investigate the potential (85) in the complete range of parameters. As before, we shall assume equality of the mass parameters for the two independent directions.

The potential is a generalization of the Hénon–Heiles potential investigated in detail earlier in the paper, but, in contrast to it, the motion in the potential (85) is finite for all energies. This is particularly important in the quantum case, in which the potential (85) ensures at all energies the existence of stationary (and not quasistationary, as in the case of the Hénon–Heiles potential) states. In addition, the potential of quadrupole vibrations is, in general, a potential with several local minima, this giving an extra interest to the study of the connection between the nature of the dynamics and the geometry of the potential-energy surface.

We now investigate the family of potential functions $U(x,y;a,b,c)$, using for this the methods of catastrophe theory.[23] The symmetry properties of the potential (80), which were studied in detail in Ref. 6, make it possible to limit the study of the potential-energy surface to the special case $U(a_0,a_2=0)$: All the critical points of the potential lie either on the line $a_2 = 0$ $(x = 0)$ or on lines obtained from it by an appropriate symmetry transformation. Without loss of generality, the parameter b can be assumed to be positive—the substitution $b \to -b$ corresponds to the mirror transformation $y \to -y$.

The set of solutions of the system of equations

$$U'_x = 0; \quad U'_y = 0; \ \det\hat{S} = 0 \tag{87}$$

serves in the parameter space as a separatrix dividing it into regions I, II, and III, in each of which the potential function is structurally stable. On the transition through the separatrix $b^2/ac \equiv W = 16$ and $a = 0$ the number and nature of the critical points change. Figure 9 shows profiles $U(x=0,y)$ of the potential (85) at the most characteristic points of the space of the parameters $(a,b,c = \text{const})$.

We consider briefly the structurally stable regions of the parameter space. Region I $(0 \leqslant W < 16)$ includes potentials that have a single extremum—a minimum at the origin. Analysis of the Gaussian curvature of the potentials that lie in this region permits its division into three subregions. In the first, $0 < W < 4$, the Gaussian curvature of the potential-energy surface is everywhere positive, and in accordance with the scenario of stochastization that relates the occurrence of local instability to entry into a region of negative

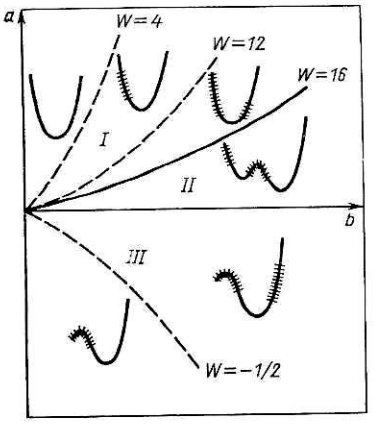

FIG. 9. Profiles of the potential $U(x=0,y)$ of the potential-energy surface for the most characteristic points of the parameter space. The regions of negative curvature are hatched.

curvature of the potential-energy surface the motion is expected to be regular. For $4 < W < 12$, a region of negative Gaussian curvature is localized at $y < 0$ in the interval

$$-\frac{1}{4}\frac{b}{c}\left(1+\sqrt{1-\frac{4}{W}}\right) < y < -\frac{1}{4}\frac{b}{c}\left(1-\sqrt{1-\frac{4}{W}}\right). \tag{88}$$

For $12 < W < 16$, a region of negative curvature also appears at $y > 0$ in the interval

$$\frac{1}{12}\frac{b}{c}\left(1-\sqrt{1-\frac{12}{W}}\right) < y < \frac{1}{12}\frac{b}{c}\left(1+\sqrt{1-\frac{12}{W}}\right). \tag{89}$$

The energies on the zero-curvature line in the section $x = 0$ of the potential-energy surface for values of W in the interval $4 < W < 16$ are shown in Fig. 10. Region II $(W > 16,\ a > 0)$ includes potentials with two (for $x = 0$) minima, one of which, at $x = 0, y = 0$, corresponds to a spherically symmetric equilibrium shape of the nucleus, while the second corresponds to a deformed nucleus. These two minima are separated by a saddle point, in the neighborhood of which the Gaussian curvature of the potential-energy surface is negative. Finally, on the transition through the separatrix $a = 0$, which separates regions II and III, we encounter potentials that describe nuclei which are deformed in the ground state and do not have even a quasistable spherical excited state. Region III can be divided into two subregions, the boundary $W = -\frac{1}{2}$ between which is the locus in the parameter space of the points at which the two eigenvalues of the stability matrix vanish simultaneously:

$$a + 2by + 4cy^2 = 0; \quad a - 2by + 12cy^2 = 0. \tag{90}$$

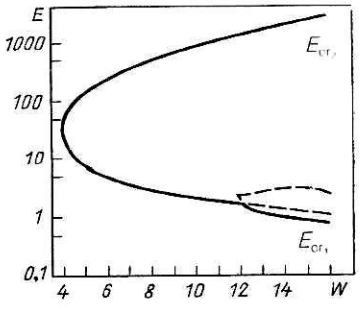

FIG. 10. Energies on the zero-curvature line in the section $x = 0$ of the potential-energy surface for values of W in the interval $4 \leqslant W \leqslant 16$. The region between the lower (E_{cr_1}) and upper (E_{cr_2}) critical energies correspond to the region of classical chaotic motion $(a = 1.0,\ c = 0.01)$.

This region includes the so-called γ-unstable nuclei, whose potential energy does not depend on γ.

We now turn to an analysis of numerical solutions of the equations of motion in the potential (85). For values of the parameter W in the interval $0 < W < 4$ all solutions of the equations of motion are regular. We recall that in this case the Gaussian curvature of the potential-energy surface is everywhere positive. In the interval $4 < W < 16$ we observe a gradual transition from quasiperiodic motion at low energies to chaotic motion at energies which make the regions of negative Gaussian curvature accessible. In region II ($W > 16$), where the deformation potential has several local minima, the numerical solutions of the equations of motion exhibit the mixed behavior already described for umbilic catastrophes, namely, in the central minimum and in the minimum corresponding to the deformed ground state different dynamical regimes are observed at an energy below the saddle energy. Poincaré maps illustrating this behavior for a potential in region II with parameters that ensure equal depths of the central minimum and the peripheral minimum are shown in Fig. 11. Finally, for $a < 0$ in the subregion $-\frac{1}{2} < W < 0$, where there is no negative curvature, all solutions of the equations of motion are regular, while in the subregion $W < -\frac{1}{2}$ chaotic motion replaces regular motion at sufficiently high energies.

As regards the critical energies of the transition to chaos, they exhibit the following clearly distinguishable behaviors:

1) for potentials with one central minimum ($0 < W < 16$), the critical energy is equal to the energy determined by the negative-curvature criterion for all values of the parameters;

2) in the case of potentials with several local minima

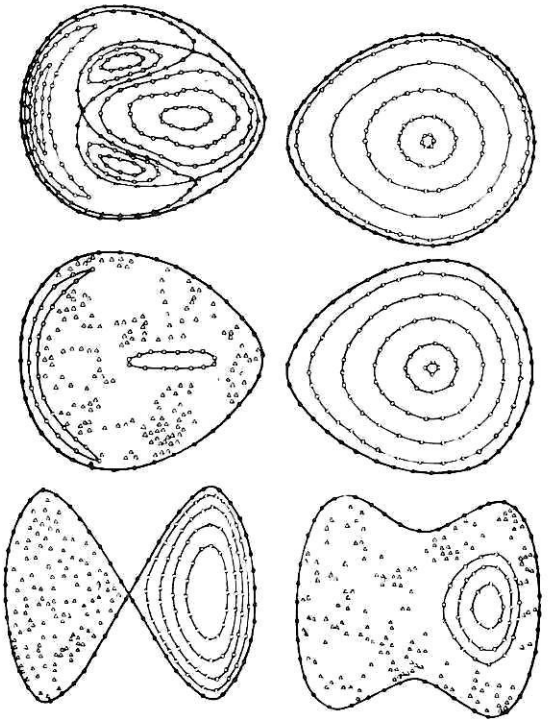

FIG. 11. Poincaré maps for motion in the potential in the region (see Fig. 9) II with parameters that ensure equal depths of the minima for different energies: $E = 0.44E_s$, $0.65E_s$, E_s, $2E_s$ (E_s is the saddle-point energy).

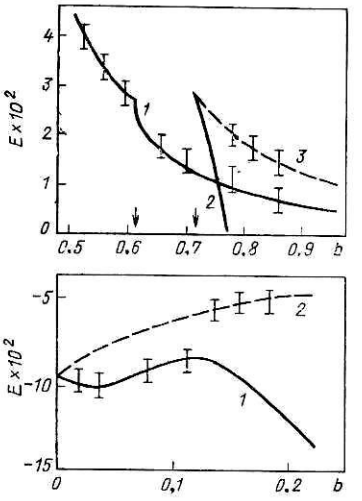

FIG. 12. Critical energy for different values of the parameters of the potential (85) ($a = 0.125$, upper figure; $a = -0.125$, lower figure) obtained on the basis of Poincaré maps. The continuous curves show the critical energies obtained using the negative-curvature criterion, and the broken curves show the saddle energies.

($W > 16$), the critical energy for a central well possessing several elliptic fixed points in the Poincaré map (see Fig. 11) is equal to the energy found by the negative-curvature criterion; for minima corresponding to nonspherical equilibrium states and possessing only one elliptic fixed point, the critical energy is equal to the saddle energy;

3) an analogous relation between the number of fixed elliptic points and the critical energy of the transition to chaos also holds for $a < 0$.

Figure 12 shows the critical energies of the transition to chaos for a potential of quadrupole vibrations ($a = \pm 0.125, c = 0.25$), determined by the negative-curvature criterion (continuous curve) and by analysis of the Poincaré maps. The arrows indicate the values of the parameter b corresponding to $W = 12$ and $W = 16$. Thus, for the potential of quadrupole vibrations too the method of determining the critical energy used in the analysis of motion in the potentials of the umbilic catastrophes is effective.

Using the parameters of the deformation potential calculated in Ref. 29, we made[30] an analysis of the classical phase space of a Hamiltonian of quadrupole vibrations that includes terms of sixth degree in the deformation for the isotopes ^{74,76,78,80}Kr. The large experimental values of the energies of the first 2^+ states for the nuclei ^{74,76}Kr indicate a spherical shape of the nuclear surface, whereas the probabilities of the $2^+ \to 0^+$ electromagnetic transitions and the very small energies of the first rotational states (converted to the same number of nucleons, this energy for the isotope ^{74}Kr is significantly less than the lowest of the known energies for ^{240}Pu: 42.8 keV) indicate the possibility of "superdeformation." These data are regarded as experimental confirmation of theoretical predictions[31,32] of the possibility of the coexistence of shapes. In superdeformed nuclei nonlinear effects associated with the geometry of the potential-energy surface must appear already at relatively low excitation energies. Inclusion in the formalism of expansion terms of higher order in the deformation leads to a significantly more complicated geometry of the potential-energy surface. As can be seen from Fig. 13, for all the considered isotopes of krypton we find potential-energy surfaces having a complicated topology with many local minima.

For all the local minima of the various isotopes of krypton the critical energies of the transition to chaos were determined by numerical solution of the equations of motion. As

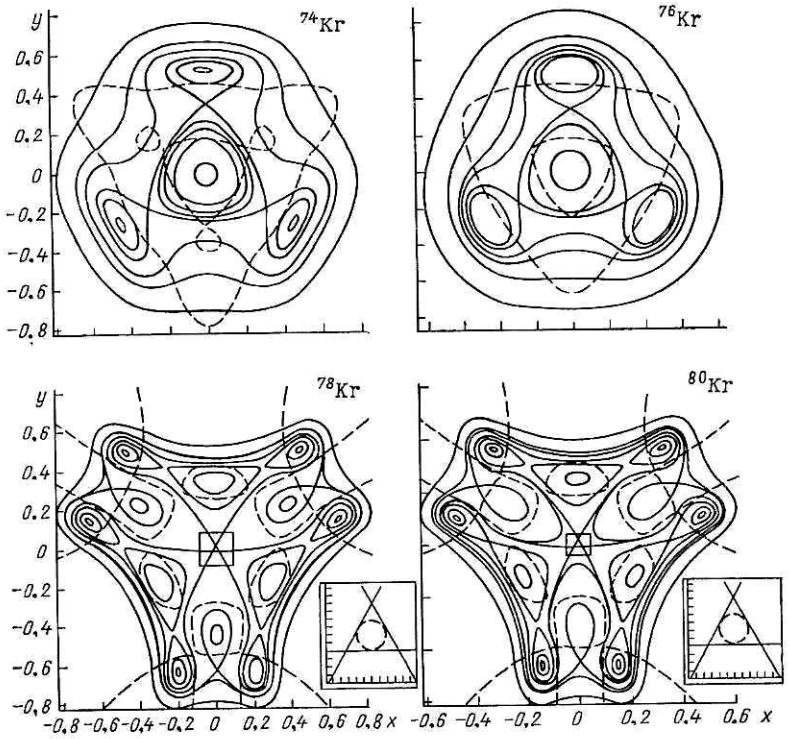

FIG. 13. Potential-energy surfaces of krypton isotopes (the broken curves show the lines of zero curvature).

for the potentials of fourth degree in the deformation considered above, the critical energies are, depending on the topology of the Poincaré maps at low energies, equal with good accuracy to either the minimal energy on the line of zero Gaussian curvature or the saddle energy.

In connection with the discussion of the critical energy of the transition to chaos determined by the negative-curvature criterion, we follow the change in the sign and in the absolute value of the Gaussian curvature for the potential-energy surface of ^{74}Kr and of the equivalent fourth-order potential (85) with parameters chosen to make the extrema of these two potentials and the values of the energies at them coincide. Figure 14 shows the Gaussian curvature $K(x=0,y)$ of the potential-energy surfaces of ^{74}Kr and the equivalent potential. It can be seen that the region of negative curvature of the latter occupies a significantly larger region of space and has a value for $y>0$ an order of magnitude greater than for the potential-energy surface of ^{74}Kr. The measure of the separation of the classical trajectories leading to the occurrence in the system of stochastic properties is determined by the size of the region and the absolute value of the negative Gaussian curvature. This circumstance permits a qualitative understanding of the reason for the transition to chaos for the quadrupole vibrations in the ^{74}Kr nucleus at comparatively higher energies than in the equivalent potential—the factors that determine the chaotic nature of the motion in the ^{74}Kr nucleus are strongly suppressed.

The comparatively small region of space in which the negative Gaussian curvature of the potential-energy surface of the isotope ^{74}Kr is concentrated also determines the nature of the motion at energies appreciably exceeding the saddle energy that separates the central minimum of the surface from the side minima. Figure 15 shows the fraction S (%) of

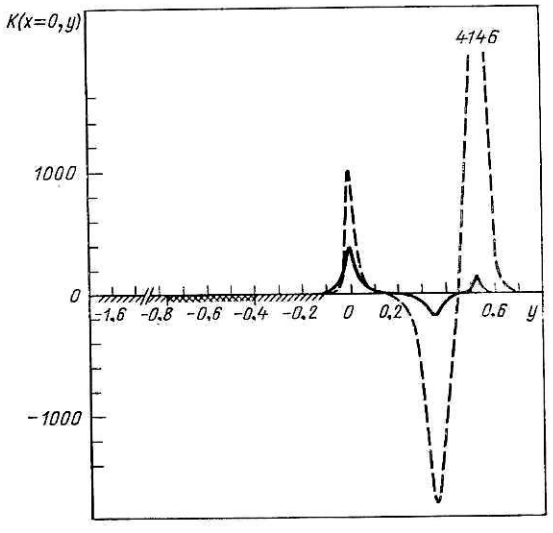

FIG. 14. profiles of the Gaussian curvature $K(x=0,y)$ of the potential-energy surface with allowance for the deformation terms of sixth order (continuous curve) and only the terms of fourth order (broken curve). [The values of the function $K(x=0,y)$ in the hatched region of the y axis are in the range 0.1–10 ^{4}.]

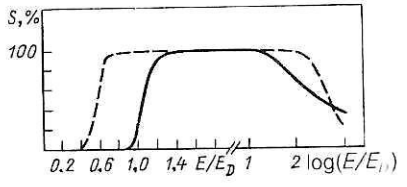

FIG. 15. Dependence of the traction S (%) of the phase space occupied by chaotic trajectories on the energy of the system. The continuous curve corresponds to the potential of quadrupole vibrations with allowance for deformation terms of sixth order; the broken curve corresponds to allowance for only the terms of fourth order.

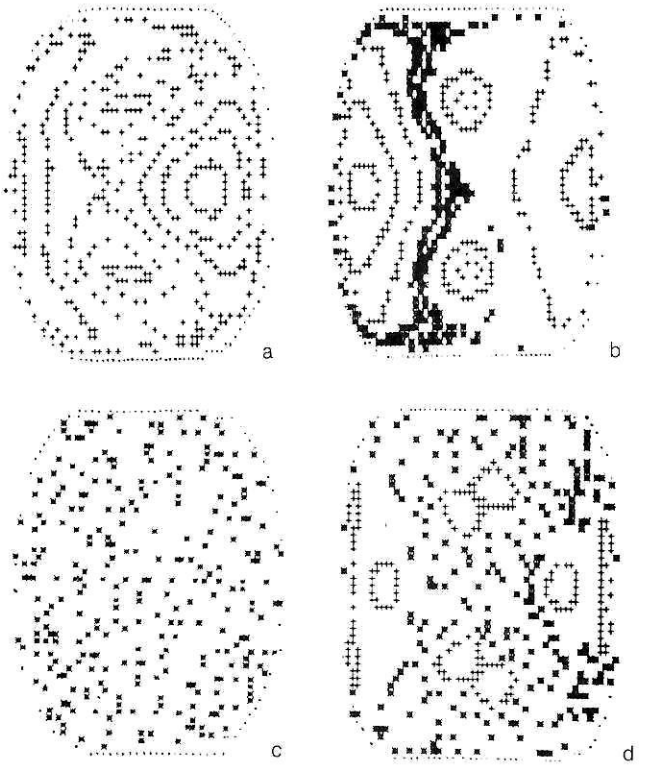

FIG. 16. Poincaré maps illustrating the restoration of regular motion in potentials of quadrupole vibrations of fourth order in the deformation (a,c) and sixth order (b,d): (a) and (b) at energy $E = 10\,000\,E_D$; (c) and (d) at $E = 100\,E_D$.

the chaotic trajectories among all the considered trajectories as a function of the energy for motion in the deformation potential of the ^{74}Kr isotope and in the equivalent fourth-order potential. It can be seen from the figure that for the krypton nucleus the critical energy of the transition to chaos is approximately equal to the saddle energy. With increasing energy 100% chaos sets in, in both potentials. However, at energies appreciably exceeding the saddle energy the regular nature of the motion is restored for both the ^{74}Kr nucleus and the equivalent potential. This new transition is illustrated by the Poincaré maps at high energies shown in Fig. 16. The earlier appearance of the regular motion at the high energies for the quadrupole vibrations of the surface of the ^{74}Kr nucleus compared with the vibrations in the equivalent potential can, as at low energies, be explained by the smaller absolute value of the negative Gaussian curvature and the greater degree of its localization. We emphasize that a similar restoration of regular motion at high energies must occur for any potential with a localized region of negative Gaussian curvature. In particular, it occurs for the isotope ^{76}Kr. But for the isotopes ^{78,80}Kr the negative curvature is not localized in a small spatial region, and therefore in this case regular motion is not restored at the energies accessible in the numerical calculations.

Concluding our study of the dynamics of autonomous two-dimensional Hamiltonian systems with polynomial potentials, we briefly formulate the main results that relate to the determination of the critical energy of the transition from regular to chaotic motion:

1) for any local minimum, the critical energy of the transition to chaos is either equal to the minimal energy on the line of zero Gaussian curvature,

$$E_{cr} = U_{\min}\ (K = 0), \tag{91}$$

or equal to the saddle energy E_s,

$$E_{cr} = E_s; \tag{92}$$

2) in a local minimum with a single saddle point chaos commences only on attainment of the saddle energy, which exceeds $U_{\min}\ (K = 0)$;

3) in the remaining cases, the possibility of applying the negative-curvature criterion is governed by the topology of the Poincaré map at low energies;

4) for potentials with a localized region of negative Gaussian curvature a return to regular motion is observed at high energies, and the critical energy of this second transition is determined by the upper boundary of the region of negative curvature.

DYNAMICAL CHAOS AND INDUCED FISSION

During an almost half-century history the process of induced fission has been studied by very different methods. Any progress in the understanding of nuclear structure was immediately reflected in fission physics. For example, the change in the widely accepted ideas about the existence of a shell structure in strongly deformed nuclei[33] led to a radical revision of the structure of the fission barrier and permitted the explanation of numerous critical experiments.

In this section, we wish to draw attention to the circumstance that stochastization of the collective motion at high excitation energies permits a reexamination of the dynamics of penetration through a multidimensional potential barrier, which plays a decisive part in the problem of induced fission.

The process of induced fission of nuclei can be represented geometrically as the motion of the representative point along some trajectory from the minimum of the deformation potential, corresponding to the ground state of the nucleus, through the saddle point into the fragment valley. The stability of such motion is largely determined by the geometry of the potential-energy surface. Thus, the existence, on the surface of the deformation potential, of a finite region of negative curvature near saddles leads to exponential separation of initially neighboring trajectories, i.e., to instability of the motion. Indeed, by means of the Maupertuis variational (least-action) principle[34] the trajectories of a dynamical system can be represented by the geodesics of some Riemannian metric defined in the part of the configuration space in which the potential energy does not exceed the total energy. Let us consider two geodesics emanating from a single point in a region of negative Gaussian curvature: $K(x,y) < 0$. In the case of a subsequent intersection, these geodesics would form a geodesic dihedron that in accordance with the Gauss–Bonnet theorem must have a sum $\alpha + \beta$ of the internal angles equal to

$$\alpha + \beta = \int K\ (x,\ y)\ d\Omega, \tag{93}$$

where $d\Omega$ is the element of surface. Since $K < 0$, we must have $\alpha + \beta < 0$. Therefore, a geodesic dihedron, for which $\alpha + \beta > 0$, is impossible in this case. Thus, in a region of negative curvature initially neighboring trajectories (for a definite choice of the metric) separate. This separation is exponential, since all solutions of the Jacobi equation for the

normal deviations on a manifold of negative curvature increase with motion along a geodesic not slower than an exponential of the traversed path for which the exponent is equal to the square root of the modulus of the curvature with respect to the two-dimensional direction for which this modulus is smallest.[7] A measure of the resulting instability is the characteristic path length S_* over which initially neighboring geodesics separate by a factor e, i.e.,

$$S_* = |K|_{\min}^{-1/2}. \tag{94}$$

It was shown in Refs. 35 and 36 that exponential instability of the geodesics on a manifold of negative curvature leads to stochastization of the corresponding geodesic flow in the phase space. We emphasize once more that it is only for the choice of a definite metric (the Maupertuis metric) that the result on the stochastization of the phase flow in the region of negative curvature is rigorous. Application of the negative-curvature criterion directly to the solutions of the Hamiltonian equations of motion requires care and is truly effective only in conjunction with a numerical experiment.

In a region of global stochasticity in which integrals of the motion restricting the behavior of the system do not exist, it is natural to replace the description of the dynamics of the system in terms of equations of motion by a statistical description. In particular, the diffusion approximation can be used to describe the phase of passage in the fission process through the region of negative curvature near the saddle of the deformation potential.[37] The quantity S_* introduced above is to be regarded as the step (length) of such diffusion. Then the diffusion coefficient is

$$D = \bar{V} S_*, \tag{95}$$

where $\bar{V}$ is the mean velocity of the motion of the representative point over the surface of the deformation potential in the region with $K<0$. The characteristic time τ_* of random walk of the representative point over a region of negative curvature with linear dimension L is

$$\tau_* = L^2/D \tag{96}$$

provided that $S_* \ll L$, an inequality that serves as a criterion for the applicability of the considered approximation.

We use the scheme described above to estimate the time delay associated with the passage through the region of negative curvature near the saddle point of the deformation potential of a fissioning nucleus.[38] For this purpose, it is sufficient to use the simplest phenomenological model of the nucleus—the liquid-drop model. In this model, the existence of a saddle point is due to competition between the Coulomb and surface forces. For deformations that preserve the axial symmetry, the equation of the nuclear surface is

$$R(\theta) = R_0 \left[1 + \sum_{\lambda=2}^{\infty} \alpha_\lambda(t) P(\cos\theta)\right]. \tag{97}$$

We are interested only in the local characteristics of this surface near the saddle point, where the deformation energy is

$$U_{\text{def}} = \hat{U}_{\text{def}} + \frac{1}{2} \sum_{\lambda\lambda'} C_{\lambda\lambda'} (\alpha_\lambda - \hat{\alpha}_\lambda)(\alpha_{\lambda'} - \hat{\alpha}_{\lambda'}). \tag{98}$$

The quantities $\hat{U}_{\text{def}}$, $\hat{\alpha}_\lambda$, and $\hat{\alpha}_{\lambda'}$ can be calculated directly at the saddle point, $C_{\lambda\lambda'}$ is the matrix of rigidity coefficients, whose eigenvectors represent the independent collective modes (stable and unstable) of the fissioning nucleus, and the eigenvalues C_λ directly determine the diffusion step

$$S_* = \bar{v}(\omega_\lambda \omega_{\lambda'})^{1/2}, \tag{99}$$

where

$$\omega_\lambda = (|C_\lambda|/B_\lambda)^{1/2}, \quad B_\lambda = \rho R_0^5/\lambda, \tag{100}$$

ρ is the density of the nucleus, and R_0 is its radius.

As the calculations of Ref. 39 show, for fissility parameter $0.39 < x < 1$ all the rigidity coefficients apart from C_2 are positive. The limiting value $x \simeq 0.39$ is a bifurcation point, below which there exists a family of saddle points of asymmetric shape. Among the stable modes, the mode with $\lambda = 4$ has the minimal rigidity. Therefore, in accordance with (94) and (99)

$$S_* = v(\omega_2 \omega_4)^{-1/2}. \tag{101}$$

For a numerical estimate we use the values of the rigidity coefficients obtained in the study of Ref. 40. Setting $\bar{v} = \sqrt{2E_F/M}$, where E_F is the threshold energy, $L \sim R_0$, for nuclei with fissility parameter $x \sim 0.8$ we finally obtain

$$\tau_* = \frac{L^2}{D} = \left(\frac{L}{v}\right)\left(\frac{L}{S_*}\right) \sim 10^2 \frac{R_0}{\bar{v}}. \tag{102}$$

Thus, the stochastization of the phase flow in the region of negative curvature of the potential-energy surface can significantly increase the time of passage through this region compared with the transit time $L/\bar{v}$ under the condition $\sim S_* \ll L$.

We recall that the standard analysis of induced fission is based on the well-known Bohr–Wheeler formula,[41] but experimentally observed deviations from this formula[42] stimulated some theoretical studies (see Ref. 43) based on the ideas of Kramers,[44] who had used the diffusion mechanism to describe monomolecular chemical reactions. Kramers's theory makes it possible to estimate the time τ of formation of a quasisteady flow through the barrier by relating it to a coefficient of nuclear friction. At large τ neutron decay will compete more effectively with the fission process, and this will lead to a decrease of the effective fission probability compared with the value predicted by the Bohr–Wheeler formula. The occurrence of diffusion through the multidimensional potential barrier on account of exponential instability of the trajectories in the region of negative curvature (without a source of a random force) is an alternative to the phenomenological diffusion of Kramers.

Similar time delays due to the occurrence of fractal structures for trajectories that pass near saddles occur in multidimensional potential scattering.[45]

QUANTUM MANIFESTATIONS OF CLASSICAL STOCHASTICITY

The important progress in the understanding of the nonlinear dynamics of classical systems stimulated numerous attempts to include the concept of stochasticity in quantum mechanics. The essence of the problem is that, on the one hand, the energy spectrum of any quantum system that executes a finite motion is discrete and, therefore, its evolution is quasiperiodic, while, on the other, the correspon-

dence principle requires the possibility of transition to classical mechanics, which possesses not only regular but also chaotic solutions. Some important results in the direction of the resolution of this obvious contradiction have already been obtained.[1,46,47] However, even before the complete solution of the problem a restricted version of it is worth considering, namely, the search for special features in the behavior of quantum systems whose classical analogs (classical systems with the same Hamiltonian) exhibit chaotic behavior.

The first attempts to find manifestations of classical stochasticity in quantum systems were associated with the study of the energy spectra and stationary wave functions of nonlinear nonintegrable model systems. The spectra were studied by comparing the "exact" quantum-mechanical spectrum with its semiclassical analog. By the "exact" spectrum we mean the spectrum obtained by diagonalizing the exact Hamiltonian on a reasonably chosen basis (of course, truncated). By the "semiclassical" spectrum we mean a spectrum obtained by a certain generalization of the Bohr–Sommerfeld procedure. In some way or other the Hamiltonian is transformed to a function of only action variables (for example, using the method of Birkhoff–Gustavson normal forms), the quantization of which then permits determination of the semiclassical energy spectrum.

It appears natural to expect that in the neighborhood of the critical energy of the transition to chaos, at which the approximate integrals of the motion used to construct the semiclassical spectrum are broken up, the agreement between that spectrum and the exact spectrum should become significantly worse. We shall analyze this effect for the example of the spectrum of the quadrupole vibrations of nuclei whose classical dynamics was studied in detail in the previous section. In the region with a single extremum—a minimum at the origin ($0 < W < 16$)—we reduce to normal form all the terms of the Hamiltonian of the quadrupole vibrations up to the fourth order and obtain for the energy spectrum the expression

$$E(N,\ L) = N + 1 + \frac{b_2}{12}[7L^2 - 5(N+1)^2 + 1] + \frac{c}{2}[3(N+1)^2 - L^2 + 1], \quad (103)$$

$$N = 0,\ 1,\ 2\ \ldots;\quad L = \pm N,\quad \pm(N-2)\ \ldots$$

Figure 17 shows the difference between the exact energy levels and those calculated in accordance with the expression (103) for the case $W = 13$, $E_{cr} = 10$. It can be seen from the figure that the semiclassical formula in the region of energies in which the classical motion is regular ($E < E_{cr}$) reproduces very well the exact quantum-mechanical spectrum. On the transition to the chaotic region ($E \gtrsim K_{cr}$), the difference increases sharply.

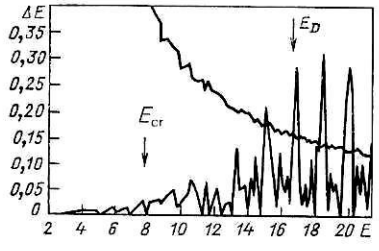

FIG. 17. Difference ΔE between the exact quantum-mechanical energy levels and the semiclassical levels (103) for the Hamiltonian of quadrupole vibrations with parameters $W = 13$, $c = 0.001\,35$, $a = 1$ ($E_{cr} = 10$). The upper curve is the mean value of the distances between neighboring levels.

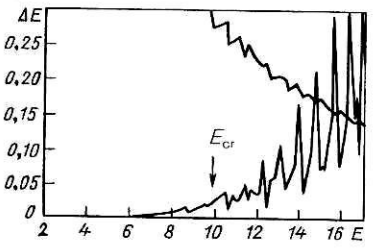

FIG. 18. The same as in Fig. 17 but for the Hénon–Heiles Hamiltonian with parameter $b = 0.1$ ($E_{cr} = 8.3$, $E_D = 16.7$).

Setting $c = 0$ in the expression (103) we can obtain the energy spectrum of the Hénon–Heiles Hamiltonian. In this case too, as can be seen from Fig. 18, the agreement between the semiclassical and exact spectra rapidly deteriorates on the transition through the value of the classical critical energy.

With regard to the more complicated problem of the behavior directly of the exact spectrum in the neighborhood of the critical energy, unanimity has not yet been achieved.[48-50]

To find the quantum manifestations of classical stochasticity in which we are interested, we can go further than study of the properties of the stationary states and consider quantum objects whose classical analogs directly exhibit stochastic behavior. Such objects, in particular, are wave packets originally localized at certain points of the phase space. To construct such wave packets, one uses[48] coherent states of the harmonic oscillator, which permit the introduction of a semiclassical phase space with density

$$\rho_\Psi(\alpha) = |\langle \alpha \mid \Psi \rangle|^2 = \rho_\Psi(\mathbf{q},\ \mathbf{p}). \quad (104)$$

The density $\rho_\Psi(\alpha)$ is the analog of the ordinary classical density and satisfies an equation of motion that in the leading order in $\hbar$ is identical to the Liouville equation.

Diagonalization of the Hamiltonian on the basis of the oscillator wave functions gives rise to a set of coefficients $C(N,L)$:

$$|E\rangle = \sum_{NL} C(N,\ L)\,|N,\ L\rangle. \quad (105)$$

This same set of coefficients permits the construction of a phase density for the stationary states,

$$\rho_E(\mathbf{q},\ \mathbf{p}) = |\langle \alpha(\mathbf{q},\ \mathbf{p}) \mid E\rangle|^2, \quad (106)$$

since the matrix elements $\langle \alpha | NL \rangle$ are well known.[51] In the two-dimensional case, the phase density for the given stationary state is a function of the four variables q_1, p_1, q_2, p_2 which determine the original localization of the wave packet in the phase space. A convenient way to study the phase density of stationary states is to plot contour charts for different sections. These have become known as quantum Poincaré sections.

We now consider the time evolution of wave packets that at the initial time form a coherent state localized at a definite point of the phase space:

$$|\Psi(t = 0)\rangle = |\alpha\rangle. \quad (107)$$

The time evolution of such a wave packet is determined by the expression

$$|\Psi(t)\rangle = \sum_E |E\rangle\langle E|\alpha\rangle e^{-iEt}. \quad (108)$$

An important characteristic of the motion is the probability of finding the system at the time t in the initial position $|\alpha\rangle$,

$$\rho(t) = |g_\alpha(t)|^2, \quad (109)$$

where the probability amplitude $g_\alpha(t)$ is the integral of the overlap of $|\Psi(t)\rangle$ with the initial wave function $|\alpha\rangle$,

$$g_\alpha(t) = \langle\alpha|\Psi(t)\rangle = \sum_E |\langle E|\alpha\rangle|^2 e^{-iEt}. \quad (110)$$

Using the definition of the phase density (104), we obtain

$$g_\alpha(t) = \sum_E \rho_E(\alpha) e^{-iEt}. \quad (111)$$

We see that the dynamics of the packet is determined by the spectrum of the initial coherent state, i.e., by the stationary states that form the original coherent state. In other words, $g_\alpha(t)$ is an almost-periodic function of the time if the energies of the eigenstates which make the dominant contribution to the density are arranged regularly. In Ref. 48 two limiting cases of the time evolution of coherent wave packets describing bound states of nonlinear nonintegrable systems were found. These two types of evolution are characterized by:

a) a quasiperiodic time evolution;

b) a rapid variation of the probabilities of population of the initial states.

Coherent states initially localized in the neighborhood of the centers of classical regular regions exhibit little dispersion and follow the classical trajectories at large times. Maximally rapid dephasing was observed for wave packets that were localized far from the centers of the regular regions.

We also consider briefly one physically interesting situation in which the quantum and classical evolutions are nearly the same.[46,47] We consider the evolution of a system over times appreciably shorter than the so-called diffusion scale t_d (Ref. 46), $t_d \sim \hbar\eta$ where η is the mean density of the energy levels. In this case, the energy uncertainty $\Delta E \gg \eta^{-1}$ is much greater than the mean distance between the levels, and the system "does not yet feel" the discrete nature of the spectrum. Therefore, over such times its evolution will be the same as in the classical limit, as numerical experiments confirm.[52,53]

Thus, the study of the classical dynamics of multidimensional Hamiltonian systems is also helpful for understanding quantum manifestations of classical stochasticity.

QUANTUM CHAOS AND STATISTICAL PROPERTIES OF NUCLEAR SPECTRA

Important correlations between features of the dynamics and the structure of the quantum energy spectrum can be obtained by a study of the statistical properties of levels. The statistical properties permit a better understanding of the fundamental properties of the system. Concepts such as temperature and entropy are important for understanding many-particle systems irrespective of whether or not we can avoid a statistical description.

We shall be interested in the local properties of the spectrum, i.e., the deviation in the distribution of the levels from mean values, in a word, fluctuations. Why must we have recourse to local properties of the spectrum? The reason is that global properties like the number of states $N(E)$ or the smoothed level density $\rho(E)$ are too crude properties, while a local property such as the distribution function of the distances between the levels is very sensitive to the properties of the potential and to the structure of the boundary. For example, it is sufficient in a square to bend one of the walls slightly for it to become dispersive, just as the classical trajectories in such a system (billiard table) become stochastic.[1] At the same time, there is a strong rearrangement of the distribution function of the distances between the levels, although the number of states $N(E)$ varies slightly or not at all.

To study the statistical properties of a spectrum, it is necessary, first, to have a sufficiently large number of levels in an interval that ensures constancy of the mean distance D between the levels and, second, to be able to identify the quantum numbers of the considered sequence of levels—the statistics of levels with the same and different quantum numbers differ strongly.

There are two main energy regions accessible for experiment.[54] The first is the low-lying region from the ground state up to energies at which the level density becomes too great and the number of competing decay channels makes it impossible to identify the spin and parity. For nuclei with $A \sim 40$, the upper limit is 7 MeV. In this interval there are about 20 levels with ten different J^π, T combinations. As a result, there are only a few levels with the same J^π, T at our disposal. The situation does not improve on the transition to heavier nuclei.

The second region lies above the threshold of neutron separation (about 15 MeV in light nuclei and about 7 MeV in heavy nuclei). The S-wave ($l = 0$) resonances are dominant in the absorption of slow neutrons with energies up to a few kilo-electron-volts. If the target, as, for example, ^{166}Er, has $J^\pi = 0^+$ in the ground state, then the final state formed as a result of neutron capture has $J^\pi = 1/2^+$. In this way it is possible to identify sequences of up to 100 levels in an energy interval of a few kilo-electron-volts. The data on proton resonances relate to lower energies. The level density in this region is significantly lower, and to obtain the same statistics it is necessary to cover a larger energy interval.

Partly because of the lack of experimental data, numerical modeling plays an important part in the study of the fluctuations of nuclear energy levels. In particular, the shell model with residual interaction makes it possible to obtain fairly large sequences of levels. The single-particle Hamiltonian determines the mean density of levels in the given energy interval, and the residual interaction fixes the position of a particular level.

Figure 19 shows histograms of the distribution of the distances between neighboring levels, $x = (E_{i+1} - E_i)/D$, taken from three different sources[55-57]: $n + {}^{166}$Er neutron resonances, isobar-analog states in the ^{49}V nucleus, and part of the spectrum of a shell model with residual interaction. Although the original spectra differed strongly, we can say that they have the same distribution of distances between neighboring levels. The histograms can be well approximated by the continuous curve

$$p(x) = \frac{\pi x}{2} e^{-\pi x^2/4}, \quad (112)$$

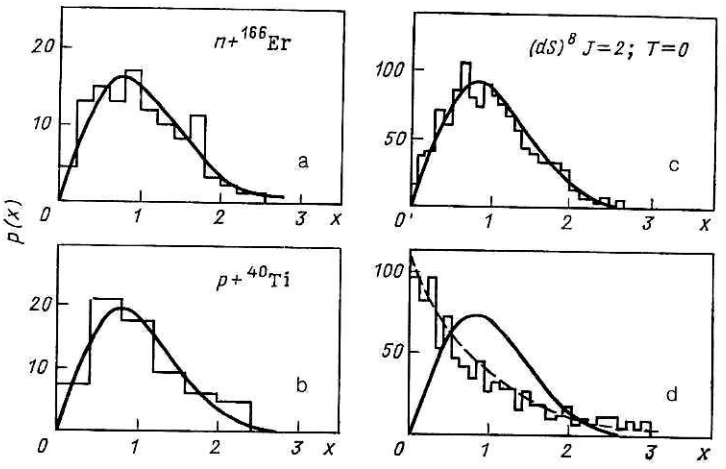

FIG. 19. Histograms of the distribution of the distances between neighboring levels constructed on the basis of all available experimental values of the energies for neutron (a) and proton (b) resonances, the spectrum of the shell model (c), and the Poisson spectrum generated by a set of random uncorrelated numbers arranged in ascending order (d).

which is called the Wigner distribution.

On the other hand, let us consider the possibility that the levels form a random sequence. Then the distances between neighboring levels have a poisson distribution (Fig. 19d):

$$p(x) = e^{-x}. \tag{113}$$

The histograms of Figs. 19a–19c and of Fig. 19d differ strongly. The nuclear spectra exhibit a "repulsion" of the levels,

$$\lim_{x \to 0} p(x) = 0, \tag{114}$$

but for the random sequence we observe a clustering of the levels—a predominance of small distances between them.

The repulsion of levels was first considered by von Neumann and Wigner[58] already in 1929. Its connection with the problem of nuclear spectra was emphasized by Wigner,[59,60] Gurevich and Pevsner,[61] and Landau and Smorodinskiĭ.[62] A history of the problem and the main studies in this direction can be found in the collection of Ref. 63.

We consider briefly some physical arguments that cast light on the phenomenon of level repulsion.[64] We consider a Hamiltonian defined in some fixed basis by means of its matrix elements. The operator H can be regarded as a vector in this space. Level repulsion can be regarded as due to the fact that a subspace for which the corresponding spectrum is degenerate has a lower dimension than the complete space of matrix elements, so that degeneracy or the weaker effect of clustering is improbable. An alternative explanation[65] is that if the Hamiltonian depends on a certain set of parameters, then level crossing when the parameters are changed can be achieved only if there exist at least two independent parameters. In the single-parameter case, one can show that repulsion at short distances is unavoidable.

So far we have discussed only pure sequences, i.e., sequences with the same quantum numbers. An example of a mixed sequence is the spectrum that results from absorption of slow neutrons by the ^{181}Ta nucleus, for which $J^{\pi} = 7/2^{+}$ in the ground state. In this case sequences of 3^{+} and 4^{+} levels are interspersed in the spectrum of neutron resonances. The level-repulsion effect is suppressed in this case by the vanishing of the matrix elements connecting states with different values of the angular momentum. The correlations between the levels become weaker, and the distribution $p(x)$ evolves to the Poisson distribution (113). If we regard different pure sequences as independent and describe each by a certain distribution, then the resultant distribution can be constructed.[61,65] Therefore, the main problem is to understand a pure sequence of levels, and all the remaining questions can be resolved in the framework of the rigorous methods of probability theory.

In the sixties, Wigner, Porter, and Dyson (see Ref. 63) constructed a statistical theory of the energy levels of complicated systems on the basis of the following hypothesis: The distribution of the energy levels is equivalent to the distribution of eigenvalues of an ensemble of random matrices of a certain symmetry. The final result for the distribution function of the distances between neighboring levels obtained in this theory has the form

$$p(x) \sim x^{\alpha} e^{-bx^2}. \tag{115}$$

The critical exponent α, which determines the behavior of the distribution function as $x \to 0$, depends on the symmetry of the matrices: $\alpha = 1$ if they are orthogonal, $\alpha = 2$ if unitary, and $\alpha = 4$ if symplectic.

The predictions of the statistical level theory (mainly the predictions for a Gaussian orthogonal ensemble of matrices) were compared in detail with the complete available set of nuclear data.[63,64] No significant discrepancies between the theory and experiment were found. In particular, ensembles of random matrices excellently reproduce the property of spectral rigidity of nuclear spectra: small fluctuations around the mean values of the number of levels in an interval of given length. Similar comparisons were made for atomic spectra.[66] Here too good agreement was obtained with the predictions for a Gaussian orthogonal ensemble, although the number of analyzed data was much less than in nuclear spectroscopy.

A quite different and fairly universal approach to the problem of the statistical properties of the energy spectra of complicated systems can be developed on the basis of the nonlinear theory of dynamical systems. Numerical calculations,[67–71] supported by solid theoretical arguments,[1,65,71] show that the main universal feature of systems that are chaotic in the classical limit is the phenomenon of level repulsion, whereas for systems whose dynamics is regular in the classical limit level clustering is characteristic. This assertion is sometimes called the hypothesis of the universal

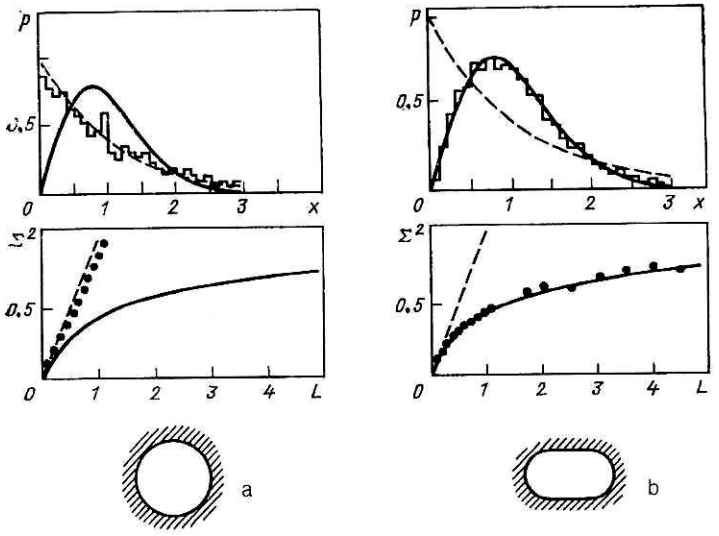

FIG. 20. Statistical properties of the energy spectra [$p(x)$ is the distribution function of the distances between neighboring levels, and $\Sigma^2(L)$ is the variance] for circular billiards (a) and "stadium" billiards (b). The continuous curves correspond to the Wigner distribution, and the broken curves to the Poisson distribution.

nature of the fluctuations of energy spectra.[67]

Among the systems whose spectra have been subjected to detailed numerical analysis, two-dimensional billiards occupy a central position. In them we have a free particle of mass m that moves freely over a plane within a certain region of arbitrary shape and undergoes elastic specular reflection at the boundary. It is convenient to investigate two-dimensional billiards for our purposes for several reasons:

1) this system has the smallest number of degrees of freedom for which chaotic motion is possible in a conservative system;

2) the classical dynamics of the system has been well studied;

3) effective methods exist for finding the billiard spectrum (the solution of the Dirichlet problem is known for boundaries of different shapes);

4) the infinite number of eigenvalues in the discrete spectrum ensures statistical reliability of the results.

For billiards with a definite shape of the boundaries, one of two extremal situations can be realized: integrable or nonintegrable. Thus, for circular billiards (Fig. 20a) the angular momentum is a second (in addition to the energy $E=p^2/2m$) integral of the motion, and such a system is integrable. A billiard table in the shape of a stadium (Fig. 20b) is the simplest stochastic dynamical system. Figure 20 (from Ref. 49) shows the statistical properties of the energy spectra (distribution function of the distances between neighboring levels and variance) of these two systems. In complete agreement with the hypothesis of a universal nature of the fluctuations of energy spectra the distribution function for the integrable system—the round billiard table—can be excellently approximated by a Poisson distribution, and the variance is a linear function of the length of the energy interval considered. In the nonintegrable case we observe level repulsion and a slow growth of the variance due to the rigidity of the corresponding spectrum. All the statistical properties of the spectrum in this case are practically identical to those of a Gaussian orthogonal ensemble of random matrices.

In contrast to billiards, in which the nature of the motion does not depend on the energy, generic Hamiltonian systems are systems with a subdivided phase space that contains both regions in which the motion is stochastic and islands of stability. How is this circumstance reflected in the statistical properties of the spectrum? Berry and Robnik,[65] and independently Bogomol'nyĭ,[73] using semiclassical arguments, showed that the distribution of distances between neighboring levels for such a system is an independent superposition of a Poisson distribution with relative weight μ determined by the fraction of the phase space with regular motion and a Wigner distribution with relative weight $\bar{\mu}(\mu+\bar{\mu}=1)$ determined by the fraction of the phase space with chaotic motion:

$$p(x)=\mu^2 e^{-\mu x}\operatorname{erfc}\left(\frac{\sqrt{\pi}}{2}\bar{\mu}x\right)+\left(2\mu\bar{\mu}+\frac{\pi}{2}\bar{\mu}^3 x\right)e^{-\mu x-\frac{\pi}{4}\bar{\mu}^2x^2}. \quad (116)$$

This is an interpolation between the Poisson distribution (113) and the Wigner distribution (112).

To trace the correlations between the statistical properties of the quantum spectrum and the nature of the classical motion, we return to quadrupole vibrations of nuclei described by the potential (85). In the region of parameter space corresponding to potentials with a single extremum ($0<W<16$) the Hamiltonian can be effectively diagonalized on a basis of harmonic-oscillator wave functions. It is convenient[48] to choose the basis states in the form

$$|N,\ L,\ j\rangle=\frac{1}{\sqrt{2}}\{|NL\rangle+j\ |N,\ -L\rangle\}, \quad (117)$$

$$N=0,\ 1,\ 2,\ \ldots;\ L=N,\ N-2\ \ldots;\ j=\pm 1.$$

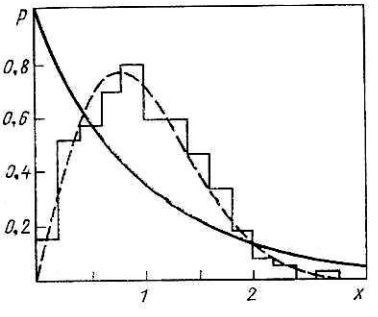

FIG. 21. Distribution of distances between neighboring levels for the chaotic region of motion in the potential of quadrupole vibrations ($W=13$, $E_{cr}=1.8$).

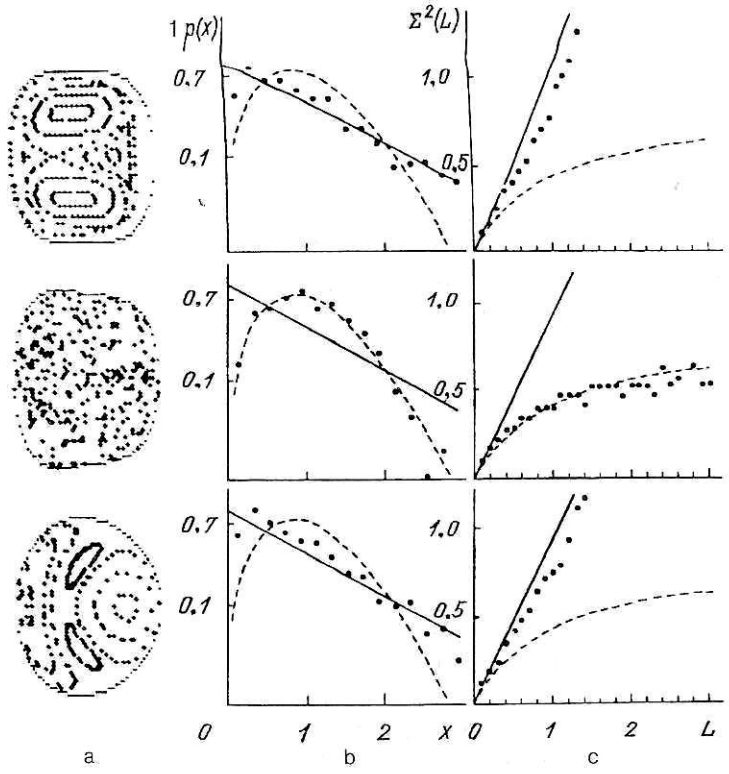

FIG. 22. Correlation between the nature of the classical motion and the statistical properties of the quantum spectrum in the triple transition (R–S–R) of the potential of quadrupole vibrations for $W = 13$: a) Poincaré maps; b) distribution $p(x)$ of distances between neighboring levels; c) variance $\Sigma^2(L)$. At the bottom, $E_{cr_1} \approx 90$ (first regular region); in the middle, $E_{cr_1} \approx 1.5$, $E_{cr_2} \approx 1895$ (chaotic region); at the top, $E_{cr_2} \approx 14.2$ (second regular region).

The symmetry of the quadrupole-vibration Hamiltonian (85) has the consequence that the matrix $\langle N', L', j' | H | N, L, j \rangle$ has a block structure. It consists of two matrices of types A_1 and A_2 [$\mathrm{Mod}(L,3) = 0, j = \pm 1$] and two identical matrices of type E [$\mathrm{Mod}(L,3) \neq 0, j = \pm 1$]. The possibility of independent diagonalization of each of these matrices permits a significant simplification of the statistics—about 300 levels of each type can be obtained with an error of about 1% in the mean distance between the levels.

Figure 21 shows the histogram of the distribution of the distances between neighboring levels for the quadrupole-vibration Hamiltonian ($W = 13$, $E_{cr} = 1.8$). In this case, all the energy levels occurring in the distribution correspond to the region of chaotic classical motion. As can be seen from the figure, the distribution $p(x)$ corresponds to the Wigner distribution, as in the case of billiards with chaotic behavior (Fig. 20b).

An even clearer correlation between the statistical properties of the quantum spectrum and the nature of the classical motion is observed in the triple regularity–chaos–regularity transition (R–S–R) that, as we noted earlier, occurs in potentials with a localized region of negative curvature. Figure 22 illustrates this correlation for three energy regions: the first regular region $E < E_{cr_1}$ (at the bottom), the chaotic region $E_{cr_1} < E < E_{cr_2}$ (in the middle), and the second regular region $E > E_{cr_2}$ (at the top). On the left we show typical Poincaré maps for these energy regions, and on the right the statistical properties of the spectrum: the logarithm of the distribution and the variance. For the chaotic region both the distribution function and the variance correspond well to the predictions for a Gaussian orthogonal ensemble. The logarithmic scale for the distribution function $p(x)$ is convenient for exhibiting this correspondence at large x. For the regular regions, the distribution function in the same scale must, in accordance with the hypothesis of the universal nature of the fluctuations of energy spectra, be a straight line (logarithm of the Poisson distribution). The calculations demonstrate agreement with this hypothesis, though for short distances between the levels a certain deviation is observed. This tendency to the formation of slight repulsion in the regular region can evidently be attributed to a small admixture of the chaotic component.

CONCLUSIONS

The most important collective phenomena in nuclei—fission and deep inelastic processes accompanying heavy-ion collisions—are collective processes with a large amplitude. A consistent theory of such processes must be an essentially nonlinear theory based on the recent achievements of the general theory of nonlinear dynamical systems. The essence of the new achievements of this theory is that under certain conditions the dynamics of a strictly deterministic system becomes indistinguishable from random dynamics. Treatment of a nucleus as a multidimensional nonlinear dynamical system reveals the possible existence in it of fundamentally new stochastic or chaotic regimes. The transition from regular to chaotic motion due to a change in the energy or other parameters of the system must have a significant influence both on the structure of the nucleus and on its interaction with external fields. In particular, the process of energy redistribution between the internal degrees of freedom is radically changed, a new approach to the description of the passage through multidimensional potential barriers is required, and the problem of the structure of the energy spectra of complicated nuclei is seen in a new light.

The future program of investigations on stochastic nuclear dynamics must include the following main directions:

1) the search for stochastic regimes;

2) the development of methods to determine the critical energy of the transition to chaos;

3) investigation of manifestations of chaotic dynamics at energies above the critical value.

In each of these directions the first steps have already been taken. Chaotic regimes have been found in the mathematical modeling of heavy-ion collisions in multipole surface vibrations of nuclei. The interpretation of negative curvature of the potential-energy surface as a source of local instability has made it possible to predict reliably the existence of chaotic regimes, and also to estimate the region of energies at which the transition to these regimes is made. The effectiveness of the approach based on analysis of the potential-energy surface is enhanced by its generality, by virtue of which the approach can be applied to a large class of nonlinear Hamiltonian systems irrespective of their particular nature.

The expected construction of γ-ray lasers by the end of the present century will make the problem of exciting stochastic regimes in nuclei by a periodic external field topical. The principle of localization of quantum chaos[47] leads in this case to nontrivial features in the absorption of the energy of an external field. Finally, allowance for dissipative effects will make it possible to include the problem of self-organization (the emergence of structure) in nuclei among the topics that are studied.

[1]G. M. Zaslavsky, *Chaos in Dynamical Systems* (Harwood Academic Publishers, Chur, 1985) [Russ. original, Nauka, Moscow, 1984].
[2]B. V. Chirikov, Phys. Rep. **52**, 265 (1979).
[3]A. J. Lichtenberg and M. A. Lieberman, *Regular and Stochastic Motion* (Springer-Verlag, New York, 1982) [Russ. transl., Mir, Moscow, 1984].
[4]M. Tabor, Adv. Chem. Phys. **46**, 73 (1981).
[5]A. Bohr and B. R. Mottelson, *Nuclear Structure*, Vols. 1 and 2 (Benjamin, New York, 1969, 1975) [Russ. transl., Mir, Moscow, 1971, 1977].
[6]J. M. Eisenberg and W. Greiner, *Nuclear Theory*, Vol. 1 (North-Holland, Amsterdam, 1970) [Russ. transl., Atomizdat, Moscow, 1975].
[7]V. I. Arnold, *Mathematical Methods of Classical Mechanics* (Springer-Verlag, Berlin, 1978) [Russ. original, Nauka, Moscow, 1974].
[8]B. V. Chirikov, Preprint 86-131 [in Russian], Institute of Nuclear Physics, Siberian Branch, USSR Academy of Sciences, Novosibirsk (1986).
[9]M. Born, Z. Phys. **153**, 372 (1958) [Russ. transl., Usp. Fiz. Nauk **69**, 173 (1959)].
[10]A. S. Umar, M. R. Stayer, and R. Y. Gusson, Phys. Rev. C **32**, 172 (1985).
[11]G. P. Berman and A. R. Kolovskiĭ, Zh. Eksp. Teor. Fiz. 87, 1938 (1984) [Sov. Phys. JETP **60**, 1116 (1984)].
[12]M. Toda, Phys. Lett. **48A**, 335 (1974).
[13]Yu. L. Bolotin, V. Yu. Gonchar, and I. V. Krivosheĭ, Khim. Fiz. **5**, 309 (1986).
[14]M. Hénon and C. Heiles, Astron. J. **69**, 73 (1964).
[15]G. Benettin, L. Galdani, and J. Strelajn, Phys. Rev. A **14**, 2338 (1976).
[16]Yu. B. Pesin, Dokl. Akad. Nauk SSSR **226**, 774 (1976).
[17]A. N. Kolmogorov, Dokl. Akad. Nauk SSSR **124**, 754 (1959).
[18]P. Brumer, Adv. Chem. Phys. **47**, 201 (1981).
[19]B. V. Chirikov, At. Energ. **6**, 630 (1959).
[20]M. I. Rabinovich and D. I. Trubnikov, *Introduction to the Theory of Vibrations and Waves* [in Russian] (Nauka, Moscow, 1984).
[21]J. Codaccioni, P. Doviel, and D. Escande, Phys. Rev Lett. **49**, 1879 (1983).
[22]A. Rechester and T. Stix, Phys. Rev. Lett. **36**, 587 (1979).
[23]T. Poston and I. Stewart, *Catastrophe Theory and Its Applications* (Pitman, London, 1978) [Russ. transl., Mir, Moscow, 1980].
[24]G. D. Birkhoff, *Dynamical Systems* (American Mathematical Society, New York, 1927) [Russ. transl., OGIZ, Moscow, 1941].
[25]F. G. Gustavson, Astron. J. **71**, 670 (1964).
[26]R. T. Swimm and J. B. Delos, J. Chem. Phys. **71**, 1706 (1979).
[27]V. Mosel and W. Greiner, Z. Phys. **217**, 256 (1968).
[28]J. M. Eisenberg and W. Greiner, *Microscopic Theory of the Nucleus* (North-Holland, Amsterdam, 1972) [Russ. transl., Atomizdat, Moscow, 1976].
[29]M. Seiwert, A. V. Ramayya, and J. A. Maruhn, Phys. Rev. C **29**, 284 (1984).
[30]Yu. L. Bolotin, V. Yu. Gonchar, V. N. Tarasov, and N. A. M. Chekanov, Preprint 88-43, Kharkov Physicotechnical Institute, Central Scientific-Research Institute of Atomic Information (1988).
[31]D. L. Hill and J. A. Wheeler, Phys. Rev. **89**, 1102 (1953).
[32]V. G. Solov'ev, *Theory of Complex Nuclei* (Pergamon Press, Oxford, 1976) [Russ. original, Nauka, Moscow, 1971].
[33]V. M. Strutinsky, Nucl. Phys. **A95**, 420 (1967).
[34]L. D. Landau and E. M. Lifshitz, *Mechanics*, 3rd ed. (Pergamon Press, Oxford, 1976) [Russ. original, 3rd ed., Nauka, Moscow, 1973].
[35]D. V. Anosov, Tr. Mat. Inst. Akad. Nauk SSSR **90**, 210 (1967).
[36]D. V. Anosov and Ya. G. Sinaĭ, Usp. Mat. Nauk **22**, 107 (1967).
[37]I. V. Krivosheĭ, Khim. Fiz. **4**, 1443 (1985).
[38]Yu. L. Bolotin and I. V. Krivosheĭ, Yad. Fiz. **42**, 53 (1985) [Sov. J. Nucl. Phys. **42**, 32 (1985)].
[39]W. Swiatecki and S. Cohen, Ann. Phys. (N.Y.) **22**, 406 (1963).
[40]G. A. Pik-Pichak, Preprint 3130 [in Russian], I. V. Kurchatov Institute of Atomic Energy, Moscow (1979).
[41]N. Bohr and A. Wheeler, Phys. Rev. **56**, 426 (1939).
[42]A. Gavron, J. Beene, and Betall Cheynis, Phys. Rev. Lett. **47**, 1255 (1981).
[43]P. Grangé, Li Jun-Qing, and H. Weidenmuller, Phys. Rev. C **27**, 2063 (1983).
[44]H. Kramers, Physica **8**, 284 (1940).
[45]C. Jung, J. Phys. A **19**, 1345 (1986).
[46]B. V. Chirikov, F. M. Israilev, and D. L. Shepelyansky, Sov. Sci. Rev. **2C**, 209 (1981).
[47]B. V. Chirikov and D. L. Shepelyanskiĭ, Preprint 85-29 [in Russian], Institute of Nuclear Physics, Siberian Branch, USSR Academy of Sciences, Novosibirsk (1985).
[48]Y. Weismann and J. Jortner, J. Chem. Phys. **71**, 1706 (1979).
[49]O. Bohigas and M. Giannoni, Lect. Notes Phys. **209**, 1 (1984).
[50]I. C. Percival, Adv. Chem. Phys. **36**, 1 (1977).
[51]J. R. Klauder and E. C. G. Sudarshan, *Fundamentals of Quantum Optics* (Benjamin, New York, 1968) [Russ. transl., Mir, Moscow, 1970].
[52]D. L. Shepelyansky, Physica **8D**, 208 (1983).
[53]G. Casati, B. U. Chirikov, F. M. Israelev, and J. Ford, Lect. Notes Phys. **93**, 334 (1979).
[54]S. Wong, *Proc. of the Como Conference on Quantum Chaos*, edited by G. Casati (1984), p. 83.
[55]H. I. Liou, H. S. Camarda, and F. Rahn, Phys. Rev. C **5**, 1002 (1972).
[56]N. S. Prochnow, H. W. Newson, and E. C. Bilpuch, Nucl. Phys. **A194**, 353 (1972).
[57]M. Soyeur and A. P. Zuker, Phys. Lett. **41B**, 135 (1972).
[58]J. von Neumann and E. P. Wigner, Phys. Z. **30**, 467 (1929).
[59]E. P. Wigner, Oak Ridge National Laboratory Report ORNL-2309 (1957), p. 59.
[60]E. P. Wigner, Columbia University Report CU-175 (TID-7547) (1957), p. 49.
[61]I. I. Gurevich and M. I. Pevsner, Nucl. Phys. **2**, 575 (1956).
[62]L. D. Landau and Ya. A. Smorodinskiĭ, *Lectures on Nuclear Theory* [in Russian] (Gostekhizdat, Moscow, 1955).
[63]*Statistical Theories of Spectra*, edited by C. E. Porter (Academic Press, New York, 1965).
[64]T. A. Brody, J. Flores, J. B. French *et al.*, Rev. Mod. Phys. 53, 385 (1981).
[65]M. V. Berry and M. Robnik, J. Phys. A **17**, 2413 (1984).
[66]H. S. Camarda and P. D. Georgopulos, Phys. Rev. Lett. **50**, 492 (1983).
[67]O. Bohigas, M. Giannoni, and C. Schmit, Phys. Rev. Lett. **52**, 1 (1984).
[68]O. Bohigas, R. V. Hag, and A. Pandey, Phys. Rev. Lett. **54**, 1645 (1985).
[69]D. Delande and J. C. Gay, Phys. Rev. Lett. **57**, 2006 (1986).
[70]T. Seligman, J. Verbaarschot, and M. Zirnbaker, Phys. Rev. Lett. **53**, 215 (1984).
[71]T. Seligman and H. Nishioka, Lect. Notes Phys. **263**, 1 (1986).
[72]M. V. Berry and M. Tabor, Proc. R. Soc. London, Ser. A **356**, 375 (1977).
[73]E. B. Bogomol'nyĭ, Pis'ma Zh. Eksp. Teor. Fiz. **41**, 55 (1985) [JETP Lett. **41**, 65 (1985)].

Translated by Julian B. Barbour